ANALYSIS OF BEST MANAGEMENT PRACTICES IMPLEMENTATION ON WATER QUALITY USING THE SOIL AND WATER ASSESSMENT TOOL (SWAT)

BY

JASON CAMPBELL MOTSINGER

THESIS

Submitted in partial fulfillment of the requirements
for the degree of Master of Science in Agricultural and Biological Engineering
in the Graduate College of the
University of Illinois at Urbana-Champaign, 2015

Urbana, Illinois

Adviser:

Professor Prasanta Kalita

Abstract

Nitrates and phosphorus are two important nutrients required for plant growth. Unfortunately, high discharge levels of these pollutants have led to major problems, affecting both health and the ecological balance. Discharged nutrients entering the Gulf of Mexico from the Mississippi River accelerate the growth of algae. When the algae die, the decomposing microorganisms consume all the dissolved oxygen in the water which thus creates a dead-zone. A vast majority of these nutrients can be traced to agricultural watersheds in the Midwest that are artificially drained in order to make the land suitable for agriculture.

The Little Vermillion River (LVR) watershed in east-central Illinois (predominately Vermillion County) is a mainly agricultural tile-drained watershed, where the dominant soil series are Drummer silty clay loam and Flanagan silt loam. Using previously collected data from the watershed outlet (1998-2000) and land management scheduling, a Soil and Water Assessment Tool (SWAT) model was calibrated and validated on a daily basis. Afterward the model was calibrated and validated using the observed data, three common Best Management Practices (BMPs) were evaluated. These BMPs include residue reduced tillage operations, vegetative filter strips, and wetlands. These BMPs were tested on a yearly (1980-2009) basis in order to determine their statistical significance and the associated pollutant reduction potential.

SWAT is able to calibrate most storm events relatively well, but large storm events are vastly underestimated on a daily basis. Base flow also tends to be underestimated. These flow problems are correlated with underestimation of daily nitrate discharge for both peak events and base flow. Since SWAT assumes that mineral phosphorus discharge occurs from watershed in surface flow only and not tile flow, mineral phosphorus could not be calibrated.

For BMPs, no tillage operation performed the best in reducing nitrates discharge from the watershed. This is thought to be caused by improved soil structure that results from not disturbing the soil. Although filter strips have been proven effective in reducing pollutants discharged from other types of watersheds, they are simulated to not be effective in LVR because most nitrates are discharged via tile drainage. Similarly, wetlands also show little effectiveness because of SWAT modeling tile flow to bypass the wetlands into the reach. Combining filter strips and wetlands with no tillage management operations results in little improvement over only no tillage management.

Acknowledgements

I would like to thank Dr. Kalita and Dr. Bhattarai for agreeing to take me on as a master's student. Their patience with me throughout this whole time has really been a Godsend. Without their continued help and support throughout all of the software troubles that I had experienced while trying to finish this, I would have given up in frustration.

Karen Wold of the Department of Rehabilitation Services (DRES) has been a big help to me throughout my undergraduate and graduate studies here at the University of Illinois at Urbana-Champaign. Her help with keeping me on track and editing the paper for grammatical errors was invaluable.

My mom, dad, and grandma have provided me with a lot of moral support throughout the time. My mom and grandma helped edit the paper, and my mom and dad helped me practice my presentation. I am happy to have them supporting me!

Without the original Little Vermillion Watershed research team collecting data, this work would not have been possible, so I am extremely grateful for their past hard work.

The SWAT development team was a big help in answering some of the problems I had with the software.

Lastly, I would like to thank Dr. Cooke for being on my committee and pointing out changes that needed to be made to my model in order to make it more valid.

Table of Contents

1. **Introduction**

The 1977 Clean Water Act was an important addition in the evolution of legislation implemented to curb water pollution (Thomas and Reed, 1980). It tasked the newly created Environmental Protection Agency (EPA) to establish maximum concentration for pollutants that would assure that water is safe for human consumption (Clean Water Act, 1972). The EPA regulates point-source polluters to help achieve this goal by setting a maximum amount of pollutants that can be discharged on a daily basis (Clean Water Act, 1972). Initially, the concern about pollution was focused on wastewater. The Clean Water Act provided incentives for wastewater reclamation and reuse (Thomas and Reed, 1980). Gradually, the EPA began studying non-point source polluters as a way to further improve water quality. Crop agriculture is a non-point source polluter. However, since farms vary in crop rotation, fertilizer application timing and rate, and conservation practices, it is not practical to measure precisely the amount each farm contributes to pollution because of monetary and time constraints. Though fertilizers are meant to add nitrogen and phosphorus to the soil in order to improve crop growth, some of the fertilizer is discharged through surface runoff and tile drainage.

Both physically-based and empirical mathematical equations have been established from research-based results, in an attempt to estimate the amount of pollutants discharged from each farm. As computing software has advanced, these equations have been packaged together in a Geographical Information System (GIS) model. GIS models require information about the soil, weather information (though this can be simulated), a digital elevation model (DEM) of the area of interest, and land management information. With this information as input, these models use mathematical equations to estimate the parameters of interest.

Nitrogen in the form of nitrates causes a number of pollution problems. The hypoxia zone in the Gulf of Mexico is largely caused by nitrates entering through the Mississippi River. In 2008, this hypoxia zone's size was measured to be 20720 km^2 (Rabotyagov et al., 2010). When nitrates enter surface water, they induce the growth of algae (Osterman et al., 2009). As the algae die, microorganisms use the available oxygen in the water to decompose them. Since the amount of dead algae is so massive due to extra nitrates, the microorganisms use all the available oxygen, leaving little to none for animal life and thus create a hypoxic or dead zone. A major source of these nitrates is discharge from agricultural operations. Nitrates can enter channel water through groundwater/base flow or surface runoff, but a major source of nitrogen is tile drainage used on poorly drained soils. Tile drainage aids in gravity drainage by enabling water to leave the soil through tiles. When nitrates enter the tiles, they are given easy access to discharge because there is minimal resistance to water flow in the tiles compared to groundwater flow; tile drainage flow also has more access to soil nitrates than surface runoff, which can only discharge nitrates from the top 10 mm of the soil matrix. An estimated 43% of nitrogen pollution and 27% of phosphorus pollution that arrives in the Gulf of Mexico can be attributed to the Upper Mississippi River Basin, an area known for the usage of tile drainage in agriculture (Aulenbach et al., 2007).

Nitrates pollution can cause problems not only for aquatic life but for human health as well. When ingested, bacteria in the stomach convert nitrates into nitrites (Lee et al., 1995). Nitrates and nitrites negatively impact the ability of the blood to carry oxygen, a condition known as methemoglobinemia; infants are more susceptible to this than adults, even with concentrations considered safe to drink, because their bodies are less able to prevent nitrites

reacting with the hemoglobin (Hegesh and Shiloah, 1982). Also in the stomach, nitrites react with amines and amide forming agents that are responsible for gastric cancer (Mirvish, 1991).

Best management practices (BMPs) are established to counteract the problems associated with increased pollutant levels due to non-point sources. Two such practices are edge of field filter strips and wetlands. Filter strips are designed to catch pollutants as they exit the agriculture field, while wetlands store the water so that microorganisms can break down the pollutants.

2. Objectives

The main objective of this is study is to calibrate and validate a watershed-scale water quality model (SWAT) for the Little Vermillion River Watershed (LVR). Another objective is to test how BMPs would improve the water quality at the watershed outlet. In order to achieve these objectives, the following research aims were proposed:

1. Analyze water-quality outlet data from Little Vermillion River Watershed to determine nutrient discharge patterns.
2. Simulate N and P discharge for LVR and compare with observed data to determine suitability of SWAT model for a tile-drained watershed.
3. Analyze the impact of various best management practices implementation on water quality at the LVR watershed outlet for recommending BMPs.

3. Literature Review

3.1. Watershed-scale quality models

Watershed-scale models simulate hydrologic processes on a watershed scale rather than a small or field scale simulation, on which other models focus (Daniel et al., 2011). These models can be subdivided, based on their processes, as either empirical-conceptual models or process-based models. Empirical models use quantitative relationships between input and output data; the transfer functions used are non-physically based, thus requiring little data to create a model (Bouraoui & Grizzetti, 2013). Trying to extrapolate the prediction of the empirical model beyond the input data may result in drastic errors, especially for heavy storm events. Process-based models use physically-based equations to simulate multiple steps that occur within the hydrologic process (Bouraoui & Grizzetti, 2013). This type of models requires a large amount of data about the watershed being modeled, making them demanding and computationally complex.

Some of the most commonly used watershed-scale hydrologic models include, but are not limited to, Annualized Agricultural Non-point Source (AnnAGNPS), Area Non-point Source Watershed Environment Response Simulation (ANSWERS-2000), Hydrological Simulation Program—FORTAN (HSPF), Soil and Water Assessment Tool (SWAT) and Water Erosion Prediction Project (WEPP) (Daniel et al., 2011). Each one of these models has its own strengths and weaknesses with the chosen model being based on what is most important for the modeler.

The AnnAGNPS model is a continuously simulated watershed-scale model capable of simulating areas the size of a small farm to an area almost twice the size of Alaska on either a daily, monthly or yearly time step, as well as being able to simulate single events (Bosch et al., 2001). The original AGNPS was an event-based model, capable of modeling pollution from

non-point sources but also from some point sources like concentrated feedlots (Young et al., 1989). However, it was only able to model areas of up to 200 km^2, with a loss in accuracy starting in watersheds exceeding 8 km^2 (Young et al., 1989). The AnnAGNPS model was developed as an expansion of the AGNPS model in order to overcome the single event limitation of AGNPS (Bosch et al., 2001). It can perform a cost-benefit analysis of common BMPs' effects on managing runoff, erosion, and nutrient management, as well as being able to analyze the long term hydrologic changes following management change (Daniel et al., 2011). The AnnAGNPS model only separates the soil into 2 layers, with the top layer being 200 mm thick and the bulk density is subject to change due to tillage; it does not simulate groundwater flow and ignores spatial variability in rainfall (Bosch et al., 2001; Daniel et al., 2011). Since the discharge of water and nitrates occurs mainly from tile drainage, AnnAGNPS would not be applicable for the watershed because it does not simulate groundwater flow.

The ANSWERS-2000 model is a physically-based process model designed for use on ungauged watersheds (Bouraoui and Dillaha, 1996). The original ANSWERS was an event-oriented model capable not only of modeling hydrology but also subsurface drainage and erosion (Beasley et al., 1980). The ANSWERS-2000 model improved upon the original ANSWERS model by giving it the ability to describe changes in soil moisture and vegetative cover between storm events (Bouraoui and Dillaha, 1996). Unlike other models like SWAT and AnnAGNPS, ANSWERS-2000 does not use the SCS CN method but instead utilizes the Green-Ampt process-based infiltration equations, allowing it to more accurately represent the effects of BMPs on flow (Bouraoui and Dillah, 1996 and 2000). The ANSWERS-2000 model can simulate flow and the discharge of phosphorus and nitrogen from watersheds (Bouraoui and Dillah, 2000). The ANSWERS-2000 model subdivides the watershed into grids (<10000 m^2) where all of the

properties are considered homogeneous (Daniel et al., 2011). The ANSWERS-2000 model does not simulate deep percolation, groundwater flow, interflow and stream base flow (Bouraoui and Dillah, 2000). It also cannot simulate channel erosion and in-stream processes (Daniel et al., 2011). Since in the study watershed groundwater plays an important role in the hydrology, ANSWERS-2000 would not be the best option.

The HSPF model is a process-based, continuous model that can simulate hydrology across both pervious and impervious land surfaces (Bicknell et al., 1997). Among the watershed-scale models endorsed by the EPA, HSPF is the most comprehensive and flexible model, being able to simulate contaminate fate as well as in-stream processes involving contaminants (Mohamoud, 2007). Like SWAT, HSPF subdivides the watershed into small, homogeneous areas called hydrologic response units (HRUs) based on uniform climate and storage capacity factors, and the model simulates the three different sediment types (Daniel et al., 2011). The model has a comprehensive representation of processes that occur within the watershed and is easily usable for a wide variety of watershed conditions. Since the model requires extensive data requirements and no comprehensive parameter guide is available, user training is required for model implementation; and the calibration process tends to be long and strenuous (Daniel et al., 2011). Requiring user training and extensive data makes HSPF not user-friendly, making modeling the study watershed difficult.

The WEPP model is another process model designed to simulate erosion (Laflen et al., 1991). It is mainly used for simulating hill slope erosion (sheet and rill) but is also applicable for hydrologic and erosion processes on small watersheds (up to $2.59*10^6$ m^2) (Daniel et al., 2011). The WEPP model operates on a daily time step, when parameters important to soil erosion, such as plant and soil characteristics, are updated; it can use either generated or simulated weather

data with the amount of runoff each day being determined by the Green-Ampt infiltration equation (Laflen et al., 1991). The WEPP model's results were found to be comparable to both the Universal Soil Loss Equation (USLE) and the Revised USLE (RUSLE) and can predict soil erosion reasonably well on either an event, monthly, or annual basis (Tiwari et al., 2000 and Zhang et al., 1996). Although its main use is to evaluate the effects of farming and land use on soil erosion and sediment delivery, WEPP has also been used to study the correlation between soil sediment and microbial transport (Daniel et al., 2011). Since this study does not look at sediment and the study watershed is slightly larger than the size WEPP can be used on as well the fact that WEPP does not model nutrients, WEPP is not the best choice for this study.

The SWAT model is another continuous physically-based process model that operates on a daily time step (Arnold et al., 1998). It is primarily used to simulate the impacts of management in ungauged watersheds (Gassman et al., 2007). Each watershed is subdivided into subbasins, which are further subdivided into homogeneous HRUs based on land use, soil, and slope. The HRUs are created based on minimum percentages that the user inputs. The SWAT model has a flexible framework, allowing it to be used on a wide variety of watersheds (Daniel et al., 2011). However, SWAT does not allow an explicit spatial representation of some BMPs, such as riparian buffers and wetlands (Daniel et al., 2011). Like other models that utilize the empirical curve number (CN) method in estimating runoff, SWAT does not reproduce measured runoff from specific storm events and has a difficult time simulating single-event storms adequately (Daniel et al., 2011). Despite these faults, the flexible and user-friendly nature of SWAT makes it the best option for this study.

3.2. Development of SWAT

The Soil and Water Assessment Tool (SWAT) is a Geographical Information System-based, continuously spatially distributed, model used to evaluate the total maximum daily load (TMDL) of watersheds as well as the effectiveness of BPMs, and operates on a daily time step; indeed, SWAT is useful for this purpose because it provides flexibility in configuring the watershed and can simulate runoff and many different pollutant levels (Arnold & Fohrer, 2005; Engel et al., 1993). The Clean Water Act requires the TMDL from a watershed to not exceed the specifications set by the EPA (Benham et al., 2011). To predict the TMDL of the watershed for various pollutants, SWAT requires spatially distributed data about the watershed to include topography, soils, land cover, land management, and weather (Douglas-Mankin et al., 2010). Currently, SWAT has the advantage over other models by being a fairly reliable model without calibration (if done correctly) (Gassman et al., 2007). It also has the ability to simulate large areas and the capability of simulating long periods of time to compute the effects of management change (Arnold et al., 1998). Unfortunately, SWAT overlooks a one-time event's effects on discharge because it operates on a daily time step. Another limitation of SWAT is its assumption that the channel geometry will remain constant throughout the simulated period.

3.2.1. Pre-SWAT

Current functions of SWAT can be traced to several models developed more than 20 years ago. These include the Chemical, Runoff, and Erosion from Agricultural Management Systems (CREAMS) model (Knisel, 1980), the Groundwater Loading Effects on Agricultural Management Systems (GLEAMS) model (Leonard et al., 1987), and the Environmental Impact

Policy Climate (EPIC) model (originally called the Erosion Productivity Impact Calculator) (William, 1990, and Izaurralde et al., 2006), with the Simulator for Water Resources in Rural Basins (SWRRB) model being the direct predecessor to SWAT (Gassman et al., 2007). First, SWRRB modified and expanded CREAMS to model large heterogeneous rural basins by allowing computations on multiple sub-basins and simulating weather, surface hydrology, crop growth, evapotranspiration (ET) and sediment movement (Arnold & Williams, 1987). Later, SWRRB was modified to predict the water table's height based on land management practices (Arnold et al., 1993). Further development of SWRRB in the late 1980s included incorporating GLEAMS to predict pesticide concentration and EPIC crop growth scenarios (Gassman et al., 2007). Routing outputs to outlet (ROTO) was developed to overcome the spatial limitations of models such as SWRRB; this physically-based and continuous model takes the outputs from other models and routes them through channels and reservoirs, with the output of one ROTO model being capable of serving as the input for another (Arnold et al., 1995). To make a more computationally efficient model, ROTO and SWRRB were merged into SWAT (Gassman et al., 2007).

3.2.2. Past Enhancement of SWAT

Since ROTO and SWRRB were combined into SWAT in the early 1990s, SWAT has undergone many major revisions and enhancements. Version SWAT 94.2 incorporated the use of hydrologic response units (HRUs) into the model (Arnold and Fohrer, 2005). Currently, HRUs are subdivided from the sub-basin with respect to land use, soils, and slopes, though slope was not included at the HRU level prior to the 2005 version of SWAT (Douglas-Mankin et al., 2010). In the SWAT 96.2 release, new management options regarding automatic fertilization and irrigation were added, as well as new equations to estimate soil water movement and

equations from QUAL2E to model pollution in streams (Arnold and Fohrer, 2005). The next three releases improved different model routines, added new management options, and expanded pollutant modeling, in addition to other enhancements. Version SWAT 2009 changed the calculation of the Soil Conservation Service's (SCS) daily Curve Number (CN) to be either a function of soil moisture or plant evapotranspiration (for use in shallow soils) and improved the modeling of vegetative filter strips and the nitrate and ammonia wet and dry deposition; in improving plant growth simulation, SWAT can now simulate multiple plant species within a community, assumes that the planting operation occurs when no land cover is growing on the HRU, and gives the user new options to change the CN throughout the year and add the CN for different management practices (Neitsch et al., 2009).

3.2.3 Legacy of SWAT: specialized versions

The SWAT model has also been modified into different specialized models. The SWIM model merges the hydraulic modeling of SWAT with the spatial distribution and nutrient modeling of MATSALU and allows for the modeling of mesoscale (100 to 10,000 km^2) watersheds (Krysanova et al., 1998). The ESWAT modification linked SWAT to MODFLOW to improve groundwater modeling (Gassman et al., 2007). The SWAT-G modification was developed for modeling in low mountain areas with large amounts of unsaturated soil water flow, using a modification of the CN method (Lenhart et al., 2002).

3.3. SWAT Equations

3.3.1 Water movement

Water is the primary cause of soil erosion and nutrient loss. When it impacts the ground via precipitation, it loosens the soil, allowing water to more easily pick up the soil particles. At first, water moves in a sheet-like pattern following the topography before developing a preferential flow path, causing rill erosion. As it moves over the surface, it mixes with water in the top 10 mm of the soil matrix, picking up some of the soluble soil nutrients in the top soil.

Surface Runoff

The SCS runoff equation is a widely used empirical model based on over 20 years of studies on the rainfall-runoff relationship and was developed in order to provide a consistent basis when estimating runoff from various land usage and soil types (Neitsch et al., 2009; Rallison and Miller, 1981). The SCS Curve Number method is defined by two equations:

$$Q_{surf} = \frac{(R_{day} - 0.2 * S)}{\left(R_{day} + 0.8 * S\right)^2} \qquad (3.1)$$

$$S = 25.4 * \left(\frac{1000}{CN} - 10\right) \qquad (3.2)$$

where Q_{surf} is the excess rainfall (mm H_2O), *R* is the day's rainfall depth (mm H_2O), *S* is the retention parameter (mm H_2O), and *CN* is the curve number (SCS, 1972). The 0.2 * S part of the equation is also called the initial extractions which include surface storage, interception, and infiltration prior to runoff. The CN is an empirical factor based on land use, treatment or land management practice, hydraulic condition, hydrologic soil group, and slope (Neitsch et al., 2009).

Normally, soils are put into one soil group, but seasonal factors could place a soil into a dual hydrologic class (Neitsch et al, 2009). The CN is adjusted by the following equations when the soil is either wet (near field capacity) or dry (near wilting point):

$$CN_{dry} = CN_{norm} - \frac{20 * (100 - CN_{norm})}{(100 - CN_{norm} + \exp[2.533 - 0.0636 * (100 - CN_{norm})])} \qquad (3.3.1)$$

$$CN_{wet} = CN_{norm} - \exp[0.0636 * (100 - CN_{norm})] \qquad (3.3.2)$$

Field capacity is the point at which gravity cannot drain any more water, and the wilting point is when plants can no longer extract water from the soil.

The following equation is used to adjust the CN for slope (standard slope is 5%):

$$CN_{norm2} = \frac{(CN_{wet1} - CN_{norm1})}{3} * [1 - \exp(-13.86 * slp)] + CN_{norm1} \qquad (3.4)$$

where the number in the subscript designates original for one and adjusted for two and *slp* is the average fraction slope for the area (Williams, 1995).

The peak discharge rate from an HRU can be found using the rational method (Neitsch et al., 2009):

$$q_{peak} = \frac{C_{runoff} * i * A}{3.6} \qquad (3.5)$$

where q_{peak} is the peak runoff rate (m^3/s), C_{runoff} is the runoff coefficient, *A* is the area of the sub basin (km^2), and *i* is the average rainfall intensity (mm/hr).

The runoff coefficient can be calculated by the equation (Neitsch et al., 2009):

$$C_{runoff} = \frac{Q_{surf}}{R_{day}} \qquad (3.6)$$

Soil Water

Vertical Movement

After rainfall enters the soil, it percolates deeper into the soil, evaporates, travels to the main channel via lateral flow, or is taken up by plants for transpiration and photosynthesis. Initially, after a rainfall in which there is surface runoff, the upper layers of soil are completely saturated. Soil properties important to the understanding of soil water movement are bulk density (dry density; ρ_b, Mg/m^3), saturated hydraulic conductivity (K_{sat}, mm/hr), soil porosity (ϕ_d, mm/mm), and particle density (density of solids, ρ_s; usually defined as 2650 Mg/m^3) (Neitsch et al, 2009).

Gravity drives the water down until it reaches the point known as field capacity. The soil water excess ($SW_{ly,excess}$) is the difference between the amount of soil water at a certain time and field capacity in a layer (mm H_2O). The percolation from one layer to a lower layer can be defined by:

$$w_{perc,ly} = SW_{ly,excess} * \left(1 - \exp\left[\frac{-\Delta t}{TT_{perc}}\right]\right) \quad (3.7)$$

where Δt is the length of the time step (hrs), TT_{perc} is the travel time for percolation (hrs), and $w_{perc,ly}$ is the daily percolation between soil layers (mm H_20) (Neitsch et al., 2009).

Travel time for the layer is found by taking the difference between saturated and field capacity water levels and dividing the difference by the saturated hydraulic conductivity of the layer (Neitsch et al, 2009). Percolation does not occur if the lower layer's soil water content is at least halfway between saturated and field capacity conditions.

Tile drainage is used on lands where water percolates very slowly. Tiles improve the percolation rate by offering some water a low resistance exit out of the soil. In doing so, it

causes the discharge of important soluble nutrients in the soil. The discharge occurs when the perched water table height (relative to the impermeable layer) is above the tile drains. Water leaving through the drains is estimated using the equation:

$$tile_{wtr} = \frac{h_{wtbl} - h_{drain}}{h_{wtbl}} * (SW - FC) * \left(1 - \exp\left[\frac{-24}{t_{drain}}\right]\right) \qquad (3.8)$$

when $tile_{wtr}$ is the amount of water leaving through the tiles on a given day (mm), h_{wtbl} and h_{drain} are, respectively, the height of the water table and tiles above the impermeable layer (mm), and t_{drain} is the time it requires to completely drain the soil above the tiles to field capacity (hrs) (Neitsch et al, 2009).

Currently, SWAT 2012 gives users the option for tile drainage to be modeled using DRAINMOD modeling routines (Moriasi et al., 2012). This modified SWAT tile drainage option uses Hooghoudt's steady-state equation to compute both drainage and sub irrigation flux and Kirkham tile drainage equation. These equations use the effective horizontal hydraulic conductivity in order to evaluate the flux between the water table level at the midway point between drains and the hydraulic head in the tiles. The Hooghoudt (1940) equation is represented as follows:

$$q = \frac{8K_e d_e m + 4K_e m^2}{C L_{tile}^2} \qquad (3.9)$$

where q is the drainage flux (mm/hr), m is the water table height above tile depth at the midpoint between tiles (mm), K_e is the effective lateral saturated hydraulic conductivity (mm/hr), L_{tile} is the distance between the tiles (mm), C is the ratio of the average flux between the tiles to the flux midway between the drains, and d_e is the equivalent depth in order to correct for convergence near the tiles (mm). "The equivalent depth (d_e) is obtained using the equations developed from

Hooghoudt's solutions by Moody (1966) as a function of L, d, and tube radius (r)" (Moriasi et al., 2012).

When the water table reaches the surface and ponded water remains for relatively long periods of time, modified SWAT switches to using the Kirkham (1957) equation:

$$q = \frac{4\pi K_e(t + b - r)}{gL} \qquad (3.10)$$

where *t* is the depth of the ponded water (mm), *b* is the depth from the surface to the midpoint of the tile (mm), *r* is the radius of the tile (mm), and *g* is a dimensionless factor determined using an equation developed by Kirkham (1957).

Horizontal Movement

In the soil, water does not simply move vertically but moves horizontally as well. In areas with soil saturated hydraulic conductivity and a shallow impermeable or semipermeable layer (like mountains), water in the soil can exit to the surface with lateral subsurface flow. The flow leaving the ground is defined by the equation (Neitsch et al., 2009):

$$Q_{lat} = 0.024 * \left(\frac{2 * SW_{ly,excess} * K_{sat} * slp}{\emptyset_d * L_{hill}}\right) \qquad (3.11)$$

where Q_{lat} is the lateral flow exiting the ground at the outlet per day (mm), K_{sat} is the saturated hydraulic conductivity (mm/hr), *slp* is the hill slope (m/m), ϕ_d is the drainable porosity (mm/mm), and L_{hill} is the length of the hill (m). Drainable porosity is defined as the amount of porosity between the total saturation and field capacity.

Base flow, or groundwater flow, maintains the main channel's water level with water from groundwater. Its steady-state response is defined by the equation (Hooghoudt, 1940):

$$Q_{base} = \frac{8000 * K_{sat}}{L_{gw}^2} * h_{wtbl} \qquad (3.12)$$

where Q_{base} being the base flow on a given day (mm), L_{gw} is the distance from the sub-basin divide (m), and h_{wtbl} is the water table height.

In SWAT, the groundwater table height is updated on a daily basis with the equation (Neitsch et al., 2009):

$$h_{wtbl,i} = h_{wtbl,i-1} * \exp[-\alpha_{gw} * \Delta t] + \frac{w_{rchg}(1 - \exp[-\alpha_{gw} * \Delta t]]}{800 * \mu * \alpha_{gw}} \quad (3.13)$$

where $h_{wtbl,i-1}$ is the previous day's groundwater table height (m), α_{gw} is the base flow recession constant, Δt is the time step (day), w_{rchg} is the recharge on the day (mm), and μ is the specific yield of the shallow aquifer (m/m).

The base flow recession can be found by the equation:

$$\alpha_{gw} = \frac{10 * K_{sat}}{\mu * L_{gw}^2} = \frac{2.3}{BFD} \quad (3.14)$$

where BFD is the number of days required for the entire watershed to contribute to base flow (Neitsch et al, 2009).

Evapotranspiration

Potential Evapotranspiration

Evapotranspiration refers to both the evaporation of water and respiration of water by plants. Potential evapotranspiration estimates the amount of evapotranspiration that would occur over a uniform area if the vegetation never ran low on available soil water (Thornthwaithe, 1948). Currently, SWAT has three methods to calculate potential evapotranspiration: the Penman-Montieth, Priestly-Taylor, and Hargreaves methods (Neitsch et al., 2009). Of these three, the Hargreaves method requires only air temperature, which is much more readily available data than solar radiation, wind speed and relative humidity (required for the other

methods), but leaving out the extra data makes it less accurate than the other methods. The Hargreaves method used in SWAT has the form (Hargreaves et al., 1985):

$$\lambda E_o = 0.023 * H_o * (T_{max} - T_{min})^{0.5} * \left(\bar{T}_{avg} + 17.8\right) \qquad (3.15)$$

where λ is the latent heat of evaporation (MJ/kg), E_o is the potential evapotranspiration (mm/day H_2O), H_o is the extraterrestrial radiation (MJ/m^2/day), and T_{max}, T_{min}, and T_{avg} are the maximum, minimum and average of daily temperature for a given day (°C). Actual evapotranspiration tends to be lower than this calculated value.

Maximum actual evapotranspiration

Before any evapotranspiration occurs, SWAT assumes all water in the canopy of the surface crop must be evaporated (Neitsch et al., 2009). Canopy storage is included in the initial extractions of the SCS method. The SWAT model projects canopy storage by the equation:

$$can_{day} = can_{mx} * \frac{LAI}{LAI_{max}} \qquad (3.16)$$

where can_{day} is the maximum amount of storage in the canopy on a given day (mm H_2O), can_{max} is the maximum storage with a fully developed leaf area index (LAI) (mm H_2O), LAI is the current LAI, and LAI_{max} is the maximum LAI for the plant.

The LAI is defined as half the surface leaf area per surface ground area (Neitsch et al., 2009). Only after all the water stored in the canopy evaporates does SWAT assume the occurrence of evapotranspiration from the soil and plants. Transpiration is assumed to follow the following equation:

$$E_t = \frac{E_o' * LAI}{3.0} \qquad (3.17)$$

where E_t is the maximum transpiration of the plant (mm/day H_2O), LAI the plant's leaf area index, and E'_o the potential evapotranspiration after all canopy stored water is evaporated (mm H_2O). The SWAT model assumes ideal growing conditions when calculating the LAI and estimating transpiration. When LAI is 3.0 or greater, E_t is equal to E'_o.

Evaporation from soil is hindered by the presence of ground cover. The soil cover index (cov_{soil}) can be found by:

$$cov_{soil} = \exp(-5 * 10^{-5} * CV) \qquad (3.18)$$

where CV is the above ground biomass and residue (kg/ha) (Neitsch et al., 2009).

The soil maximum evaporation can be found by:

$$E_s = E'_o * cov_{soil} \qquad (3.19)$$

where E_s is the maximum soil evaporation (mm H_2O) (Neitsch et al., 2009).

During periods of high water usage by vegetation, the maximum soil evaporation is adjusted by the formula:

$$E'_s = min\left(E_o, \frac{E_s * E'_o}{E_s + E_t}\right) \qquad (3.20)$$

where E'_s is the adjusted maximum soil evaporation (mm H_2O) (Neitsch et al., 2009).

For calculations, SWAT must divide the evaporation demand throughout the soil matrix based on depth. The amount of evaporation demanded up to a certain depth is estimated by the equation:

$$E_{soil,z} = E'_o * \frac{z}{z + \exp(2.374 - 0.00713 * z)} \qquad (3.21)$$

where z is the depth from the surface (m) and $E_{soil,z}$ is the amount soil evaporation demanded of the soil above the depth z (mm H_2O) (Neitsch et al., 2009).

To determine the amount demanded of a certain layer, the amount demanded above the layer is subtracted from the amount demanded from above the lower boundary of the layer. A modified version of this equation is given as follows:

$$E_{soil,ly} = E_{soil,zl} - E_{soil,zu} * esco \qquad (3.22)$$

where $E_{soil,ly}$ is the evaporation demanded of the layer (mm/day H_2O), $E_{soil,zl}$ and $E_{soil,zu}$ are the evaporation demand above the lower and upper boundaries of the layer, respectively (mm/day H_2O), and *esco* is the soil evaporation coefficient, which allows for lower layers to supply more water for the evaporation demand for lower values (Neitsch et al., 2009).

When the layer's water content is below the field capacity of the layer, the evaporation demand of the layer is modified by the equation:

$$E'_{soil,ly} = E_{soil,ly} * exp\left(\frac{2.5 * (SW_{ly} - FC_{ly})}{FC_{ly} - WP_{ly}}\right) \qquad (3.23)$$

where $E'_{soil,ly}$ is the adjusted evaporation demand of the layer (mm H_2O). In these calculations, SWAT assumes that the maximum amount of water that can be evaporated on a given day is 80% of plant available water. If the adjusted evaporation demand of the soil layer is above this, the evaporation demand becomes 80% of the plant available water (Neitsch et al., 2009).

When the water content comes closer to wilting point, it becomes more difficult to evaporate the water. When the topmost layers cannot supply the soil evaporation demand for the layer, it puts extra pressure on lower layers for more to be evaporated. Unfortunately, SWAT does not allow a lower layer to compensate for the excess demand on higher layers, thus the actual soil evaporation is underestimated by SWAT (Neitsch et al., 2009).

3.3.2. Sediment loss

The soil itself contains the nutrients as well as being the natural anchor that plants need to grow. When precipitation occurs, soil particles are broken loose from the ground, allowing for water runoff to carry soil particles away from the field. The empirical USLE is widely used to predict yearly sediment loss from water erosion. However, SWAT requires daily sediment loss and thus uses the modified USLE (MUSLE), given by the equation (Williams 1995):

$$sed = 11.8 * \left(Q * q_{peak} * A_{hru}\right)^{0.56} * K_{USLE} * C_{USLE} * LS_{USLE} * CFRG \qquad (3.24)$$

where *sed* is the sediment loss on a given day (Mg), A_{hru} is the area of the hru (ha), and K_{USLE}, $C_{USLE,}$ LS_{USLE}, P_{USLE}, and CFRG are the USLE soil erodibility, cover and management, topography, support practice, and the coarse fragment empirical factors, respectively.

Depending on the makeup of the soil matrix, some soils are more prone to water erosion than others. The K_{USLE} factor is estimated by the following equation when silt and very fine sand make up less than 70% of the soil particle size distribution (Wischmeier et al., 1971):

$$K_{USLE} = \frac{0.00021 * M^{1.14} * (12 - OM) + 3.25 * \left(c_{soil,str} - 2\right) + 2.5 * (c_{perm} - 3)}{100} \qquad (3.25)$$

where *M* is the particle size parameter, OM is the % organic matter, $c_{soil,str}$ is the soil structure code, and c_{perm} is the profile permeability factor.

The *M* factor is calculated using the percentage of soil by soil particle size (Neitsch et al., 2009):

$$M = \left(m_{silt} + m_{vfs}\right) * (100 - m_c) \qquad (3.26)$$

where m_{silt} is the % silt content (0.002-0.05 mm diameter particle size), m_{vfs} is the % very fine sand (0.05-0.10 mm), and m_{clay} is the % clay (<0.002 mm).

The % organic matter content can be estimated by multiplying the % organic carbon content by 1.72 (Neitsch et al., 2009).

The $C_{soil,str}$ factor classifies the soil based on the size of individual structure. The four main soil structure classes are platy, prismatic, block-like, and spheroidal (Neitsch et al., 2009). The classification numbers are based on the size of an individual soil structure: 1 for very fine granular, 2 for fine granular, 3 for medium or coarse granular, and 4 for blocky or massive. Each soil structure classification has different size criteria for each class. Platy and spheroidal soils have the lowest thresholds of the soil structure, while prismatic has the highest threshold.

The C_{perm} factor also is an empirical number based on the lowest saturated hydraulic conductivity in the layer. Classification numbers are: 1 for rapid (>150 mm/hr), 2 for moderate to rapid (50-150 mm/hr), 3 for moderate (15-50 mm/hr), 4 for slow to moderate (5-15 mm/hr), 5 for slow (1-5 mm/hr), and 6 for very slow (<1 mm/hr) (Neitsch et al., 2009).

The cover and management factor compares the current conditions to clean-tilled fallow conditions (Wischmeier and Smith, 1978). Currently, SWAT updates daily C_{USLE} based on the calculated growth cycle of the plant based on the equation (Neitsch et al., 2009):

$$C_{USLE} = \exp\left(\left[ln(0.8) - ln\left(C_{USLE,mn}\right)\right] * exp[-0.00115 * CV] + ln\left[C_{USLE,mn}\right]\right) \quad (3.27)$$

where $C_{USLE,mn}$ is the minimum value for C_{USLE}.

The $C_{USLE,mn}$ value is found by the equation, using the average cover and management factor ($C_{USLE,aa}$) for current land cover (Arnold and Williams, 1995):

$$C_{USLE,mn} = 1.463 * \ln\left[C_{USLE,aa}\right] + 0.1034 \quad (3.28)$$

The support practice factor empirically compares how well a specific management practice compares with a conventional row crop practice for agriculture (Neitsch et al., 2009). Some support practice factors include: contour tillage and planting, contour strip cropping, and

terraces. Contouring farming, when crops are planted along an equal elevation line, provides good protection against rainfall of low to moderate intensity, because water would not have a natural path downhill with planting hindering the flow path, but not against heavy downpours or land with a relatively steep slope. Contour strip cropping differs from regular contouring since there are alternating strips of different crops, with the P factor based on rotation. A common practice for strip cropping is alternate sections of row crops like corn with small grains like oats. Both of these methods are the most effective on 3-8% slopes (Neitsch et al., 2009). To improve the performance of these methods on steeper slopes, a series of horizontal ridges in the hillside, called terraces, are added. Terraces add horizontal ridges along the contour, equal distance apart, so that each interval is the same length. These methods cause the water movement to slow so it will drop sediment particles.

"The topographic factor, LS_{USLE}, is the expected ratio of soil loss per unit area from a field slope to that from a 22.1-m length of 9 percent uniform slope under otherwise identical conditions" (Neitsch et al., 2009). This factor is empirically derived using the equation:

$$LS_{USLE} = \left(\frac{L_{hill}}{22.1}\right)^{m} * (65.41 * [\sin(\tan^{-1} slp)]^2 + 4.56 * [\sin(\tan^{-1} slp)] + 0.065) \qquad (3.29)$$

where L_{hill} is the length of the slope (m) and *m* as an exponential term based on slope.

The *m* factor is derived using the equation (Neitsch et al., 2009):

$$m = 0.6 * (1 - \exp[-35.835 * \text{slp}]) \qquad (3.30)$$

The coarse fragment factor considers what percentage rocks are in the topmost layer of the soil profile. Rocks are large and difficult for water to carry off. The factor is calculated by the equation (Neitsch et al., 2009):

$$CFRG = \exp(-0.053 * rock) \qquad (3.31)$$

where rock is the % of rocks in the topmost layer. For the most part in agricultural areas, the % of rocks in the topmost layer is negligible, so this term can be ignored.

Groundwater and subsurface lateral flow can also contribute sediment to the main channel. Sediment lost due to this effect is found by the equation:

$$sed_{lat} = \frac{(Q_{lat} + Q_{gw}) * area_{hru} * conc_{sed}}{1000} \qquad (3.32)$$

where $conc_{sed}$ is the concentration of sediment in lateral and groundwater flow (mg/L) and sed_{lat} is the soil lost per day due to these processes (Mg) (Neitsch et al., 2009).

3.3.3. Nutrient movement

Nitrogen

Nitrogen in soil

Nitrogen is one of the key elements in the growth of plants. It is added to the soil through fertilizer, residual crop material and manure application, and microbial fixation. It leaves the soil through erosion, leeching, denitrification, plant uptake, and volatilization. The SWAT models organic and mineral nitrogen and how they react in the soil. The initial nitrate levels, which are the primary form of nitrogen that plants uptake, have an inverse exponential relationship with depth (Neitsch et al., 2009):

$$NO3_{conc,z} = 7 * \exp\left(\frac{-z}{1000}\right) \qquad (3.33)$$

where $NO3_{conc,z}$ is the initial concentration (mg/kg or ppm) of nitrates at a depth *z* (mm).

The addition of new sources of nitrogen changes this number. Bacteria can change inaccessible organic nitrogen into usable nitrates and vice versa. Assuming an organic C:N ratio of 14:1, the organic nitrogen in the layer (ppm) can be found with the equation:

$$orgN_{ly} = 10^4 * \left(\frac{orgC_{ly}}{14}\right) \qquad (3.34)$$

where $orgC_{ly}$ is the % of organic carbon in the layer (Neitsch et al., 2009).

Only part of the organic nitrogen is available for use in mineralization. This part, defined as the active layer ($orgN_{active,ly}$), is only a small fraction of all organic nitrogen (usually 2%) (Neitsch et al., 2009). Mineralization and immobilization of nitrogen are ways in which bacteria change nitrogen's form in the soil. Bacteria need a C:N ratio between 20:1 and 30:1. If it is any higher, bacteria immobilize nitrates by fixing the nitrates to soil particles. If it is any lower, then bacteria mineralize nitrogen by releasing the extra nitrogen as nitrates. For equations involving nutrient transformation in the soil, SWAT calculates a nutrient cycling temperature factor for the layer, defined by the equation:

$$\gamma_{tmp,ly} = 0.9 * \frac{T_{soil,ly}}{T_{soil,ly} + \exp\left[9.93 - 0.312 * T_{soil,ly}\right]} \qquad (3.35)$$

where $T_{soil,ly}$ is the temperature of the soil layer (°C).

When mineralization occurs, SWAT estimates it with the following equation:

$$N_{mina,ly} = \beta_{min} * \left(\gamma_{tmp,ly} * \frac{SW_{ly}}{FC_{ly}}\right)^{\frac{1}{2}} * orgN_{active,ly} \qquad (3.36)$$

where $N_{mina,ly}$ is the amount of new nitrates in the layer (kg N/ha), β_{min} is the rate coefficient for mineralization, and $orgN_{active,ly}$ is the amount of organic nitrogen in the active layer (kg N/ha) (Neitsch et al., 2009).

When bacteria cannot obtain oxygen for their processes (anaerobic conditions), they use nitrates to fulfill their metabolic needs. When they do, they reduce nitrates into either nitrogen gas or dinitrogen monoxide gas (N_2O). The SWAT model uses the following equation to determine if denitrification occurs:

$$\gamma_{sw,ly} = \frac{SW_{ly}}{FC_{ly}} \qquad (3.37)$$

where $\gamma_{sw,ly}$ is the fraction of non-gravity drained soil porosity is filled with water (Neitsch et al., 2009). If $\gamma_{sw,ly}$ is greater than or equal to 0.6, SWAT assumes denitrification occurs.

When temperature is higher, more denitrification occurs. The SWAT model estimates denitrification with the equation:

$$N_{denit,ly} = NO3_{ly} * \left(1 - \exp\left[\beta_{denit} * \gamma_{tmp,ly} * orgC_{ly}\right]\right) \qquad (3.38)$$

where $N_{denit,ly}$ is the amount of nitrogen lost to denitrification (kg/ha), $NO3_{ly}$ is the amount of nitrates in the layer (kg/ha), β_{denit} is the rate coefficient for denitrification, and $orgC_{ly}$ is the amount of organic carbon in the layer (%) (Neitsch et al., 2009).

Nitrogen in Surface runoff, groundwater flow, and percolation

Soil minerals tend to be negatively charged at normal pH. This causes them to attract positively charged cations while repulsing negatively charged anions like nitrates. As such, nitrates cannot be found in the smaller pores due to the strength of the negative charged repulsion of the soil particles. This leads to nitrates moving faster on average than soil water. The concentration of nitrates in mobile water is calculated by the equation:

$$conc_{NO3,mobile} = \frac{NO3_{ly} * (1 - \exp[\frac{-w_{mobile}}{(1 - \emptyset_e) * SAT_{ly}}]}{w_{mobile}} \qquad (3.39)$$

where $conc_{NO3,mobile}$ is the concentration of nitrates in mobile water for a given layer (kg N/mm H_2O), $NO3_{ly}$ is the amount of nitrates in the layer (kg N/ha), ϕ_e is the fraction of porosity in which anions are excluded, and w_{mobile} is the amount of mobile water in a layer (mm) (Neitsch et al., 2009).

In the top 10 mm of soil, mobile water is the sum of surface runoff, subsurface lateral/groundwater flow, and percolation. For all other layers, mobile water is the sum of the latter two (Neitsch et al., 2009). The amount of nitrates removed via surface runoff is found by the equation:

$$NO3_{surf} = \beta_{NO3} * conc_{NO3,mobile} * Q \qquad (3.40)$$

where $NO3_{surf}$ is the amount of nitrates removed via surface runoff (kg N/ha) and β_{NO3} is the nitrate percolation coefficient ($conc_{NO3,mobile}$ is only for top 10 mm). Movement of nitrates through groundwater/lateral subsurface flow and percolation is found the same way, minus the nitrate percolation coefficient for layers lower than 10 mm.

When sediment leaves the soil via surface runoff, organic forms of nitrogen leave with it, since organic nitrogen tends to be part of the soil matrix. Organic nitrogen lost due to surface runoff is estimated using the equation:

$$orgN_{surf} = 0.001 * conc_{orgN} * \frac{sed}{area_{hru}} * \varepsilon_{N:sed} \qquad (3.41)$$

where $orgN_{surf}$ is the amount of organic nitrogen lost to surface (kg N/ha), $conc_{orgN}$ is the concentration of nitrogen in the top layer (g N/Mg), and $\varepsilon_{N:sed}$ is the nitrogen enrichment ratio (Neitsch et al., 2009).

The concentration of nitrogen can be found by the equation:

$$conc_{orgN} = 100 * \frac{orgN}{\rho_b * depth_{surf}} \qquad (3.42)$$

where orgN is the total amount of organic nitrogen in the surface layer (kg N/ha) and $depth_{surf}$ is the depth of the surface layer (10 mm) (Neitsch et al., 2009).

"The enrichment ratio is defined as the ratio of the concentration of organic nitrogen transported with the sediment to the concentration in the soil surface layer" (Neitsch et al., 2009). Users can manually establish an enrichment ratio, or by default SWAT will define it with the relationship:

$$\varepsilon_{N:sed} = 0.78 * \left(conc_{sed,surf}\right)^{-.2468} \quad (3.43)$$

where $conc_{sed,surf}$ is the concentration of sediment in the surface runoff (Mg/m^3). This is the sediment lost from an HRU divided by the runoff depth and HRU area.

Phosphorus

Phosphorus in the soil

Phosphorus is another key element in plant growth, though it is found in lower amounts in the soil and has lower plant demand than nitrogen. It is found in soils as insoluble mineral phosphorus, plant-available phosphorus, and organic phosphorus. It is added to the soil through fertilizer, manure, and residual crop application. Phosphorus is removed through harvest and erosion. Under normal conditions, soluble (aka plant-available) phosphorus is at a concentration of 5 ppm, though farming practices have led it to be assumed it to be 25 ppm in the plow layer (Neitsch et al., 2009). Insoluble mineral and organic forms of phosphorus can be subdivided into active and inactive pools. The concentration of active mineral phosphorus (ppm) is found with the relationship under equilibrium conditions (Jones et al., 1984):

$$minP_{active,ly} = P_{solution,ly} * \frac{1 - pai}{pai} \quad (3.44)$$

where pai is the phosphorus availability index.

The PAI is calculated using the following relationship based on soluble phosphorus before and after fertilizer application, based on results obtained using a laboratory experiment (Neitsch et al., 2009):

$$pai = \frac{P_{solution,f} - P_{solution,i}}{fert_{minP}} \quad (3.45)$$

where $P_{solution,f}$ is the concentration of soluble phosphorus after fertilization and incubation of the soil, $P_{solution,i}$ is the concentration of soluble phosphorus initially, and $fert_{minP}$ is the amount of soluble phosphorus in the fertilizer.

The stable amount of mineral phosphorus is four times greater than the amount of active phosphorus at equilibrium, while the amount of organic phosphorus is just $1/8^{th}$ that of organic nitrogen (Jones et al., 1984, and Neitsch et al., 2009). The amount of active organic phosphorus in a layer (kg P/ha) is the same fraction of total organic phosphorus as active organic nitrogen is to total organic nitrogen. The SWAT model assumes that the mineralization of phosphorus does not occur unless the temperature of the soil layer is above 0°C. When mineralization from the active organic phosphorus to soluble phosphorus occurs, SWAT calculates it as (Neitsch et al., 2009):

$$P_{mina,ly} = 1.4 * \beta_{min} * \left(\gamma_{tmp,ly} * \gamma_{sw,ly}\right)^{\frac{1}{2}} * orgP_{act,ly} \quad (3.46)$$

where $P_{mina,ly}$ is the net amount of phosphorus mineralized (kg/ha) and $orgP_{act,ly}$ is the active amount of organic phosphorus in the layer (kg/ha).

When mineral phosphorus is not at equilibrium, phosphorus is exchanged between the stable and active mineral pools and soluble pools (Neitsch et al., 2009). The transfer of phosphorus is calculated using the following equations:

$$P_{sol|act,ly} = 0.1 * \left(P_{solution,ly} - minP_{act,ly} * \left[\frac{pai}{1 - pai}\right]\right) \qquad (3.47.1)$$

$$if\ P_{solution,ly} > minP_{act,ly} * (\frac{pai}{1 - pai})$$

$$P_{sol|act,ly} = 0.6 * \left(P_{solution,ly} - minP_{act,ly} * \left[\frac{pai}{1 - pai}\right]\right) \qquad (3.47.2)$$

$$if\ P_{solution,ly} < minP_{act,ly} * (\frac{pai}{1 - pai})$$

where $P_{sol|act,ly}$ is the amount of phosphorus transferred between the pools (kg P/ha; positive for solution to active movement), $P_{solution,ly}$ is the amount of soluble phosphorus in the layer (kg P/ha), and $minP_{act,ly}$ is the amount of active mineral phosphorus in the layer (kg P/ha).

The rate of flow of phosphorus from active mineral pool to solution is $1/10^{th}$ of the reverse reaction (Neitsch et al., 2009). When these reactions occur, the assumed slow equilibrium between active and stable mineral phosphorus no longer exists.

The following equations estimate the mass transferred between the two states (positive is transfer of mass to the stable state):

$$P_{act|sta,ly} = \beta_{eqP} * \left(4 * minP_{act,ly} - minP_{sta,ly}\right) \qquad (3.48.1)$$

$$if\ 4 * minP_{act,ly} > minP_{sta,ly}$$

$$P_{act|sta,ly} = 0.1 * \beta_{eqP} * \left(4 * minP_{act,ly} - minP_{sta,ly}\right) \qquad (3.48.2)$$

$$if\ 4 * minP_{act,ly} < minP_{sta,ly}$$

where $P_{act|sta,ly}$ is the mass transferred between the two states in the layer (kg P/ha) and β_{eqP} is the slow equilibrium constant for phosphorus (0.0006/day) (Neitsch et al., 2009).

Phosphorus in Surface Runoff, Groundwater flow, and Percolation

Within the soil, the mobility of phosphorus is very limited since the primary movement of phosphorus in soil is by diffusion; thus, a vast majority of phosphorus pollution comes from surface runoff. The SWAT model does allow for leaching of solution phosphorus; however phosphorus leaving the top 10 mm of soil is assumed to not leach any further (Neitsch et al., 2009). The SWAT model calculates the mass of soluble phosphorus in surface runoff (kg P/ha) with the equation:

$$P_{surf} = \frac{P_{solution,surf} * Q}{\rho_b * depth_{surf} * k_{d,surf}} \qquad (3.49)$$

where $k_{d,surf}$ is the phosphorus soil partitioning coefficient (m^3/Mg), which can either be user defined or calculated by SWAT.

Phosphorus transported with sediment (kg P/ha) is calculated with the equation:

$$sedP_{surf} = 0.001 * conc_{sedP} * \frac{sed}{area_{hru}} * \varepsilon_{P:sed} \qquad (3.50)$$

where $conc_{sedP}$ is the summation of the concentration of mineral and organic phosphorus (ppm) and $\varepsilon_{P:sed}$ is the phosphorus enrichment ratio (Neitsch et al., 2009).

The enrichment ratio is found with the equation:

$$\varepsilon_{P:sed} = 0.78 * \left(conc_{sed,surq}\right)^{-0.2468} \qquad (3.51)$$

where $conc_{sed,surq}$ is the concentration of sediment in the surface runoff (Mg/m^3) (Neitsch et al., 2009).

3.3.4. Vegetative Filter Strips

To reduce the amount of pollutants leaving a site through surface runoff, grass filter strips are planted in the pathway of the flow. This common practice slows the flow of runoff, resulting

in the deposition of pollutants that it has picked up. Prior studies have evaluated the effectiveness of filter strips based on the old filter strip routines. The original VFS modelling component in SWAT had a single efficiency equation for sediments, nutrients, and pesticides based on filter strip length (Fox and Penn, 2013). New routines were developed in order to improve filter strip modelling in SWAT. In order to compensate for differences in HRU sizes, shapes, and conductivity, SWAT creates a vegetative filter strip of a size corresponding to the unitless ratio of drainage area to filter strip area (White and Arnold, 2009). This ratio can be applied to multiple HRUs because the size of the filter strip will vary with the size of the drainage area. In order to measure VFSMOD's effectiveness being utilized in SWAT, White and Arnold (2009) derived results from 22 published studies in order to comparatively evaluate VFSMOD. The studies looked at that report both runoff loading and soluble phosphorus reduction percentage showed VFS with low runoff flow had soluble phosphorus reduction of over 70%. The soluble components of the nutrient reduction model have a linear relationship with runoff reduction (runoff reduction empirical equation has an R^2=0.76 for 1650 data points examined). The empirical mineral phosphorus showed a low correlation between the model and studies' data (R^2=0.27), yet the slope and intercept were both found to be statistically significant (P=0.01). Nitrate removal tended to be well over 30%, but some studies had shown a net increase in nitrate nitrogen than a removal. The empirical model for nitrate nitrogen exhibited a better fit to the data (R^2=0.67), with the both the slope and intercept being statistically significant (P<0.01). A 50-year model using this empirical model for VFS on Tipton loam soil in Kansas shows a greater sensitivity of mineral phosphorus to filter strip size than nitrates showed, which agrees with the experimental data results (White and Arnold, 2009).

The new VFS routine assumes a linear relationship between sediment reduction and total phosphorus reduction, which becomes less accurate as mineral phosphorus becomes a larger component (Fox and Penn, 2013). This tends to occur more in no-till agriculture, pasture, hay fields, and urban landscapes. On an annual basis, mineral phosphorus comprises less than 15% of the total mineral phosphorus at the outlet in the default case, making the total phosphorus reduction model valid for this watershed. However, on a monthly basis, mineral phosphorus fraction of total phosphorus becomes greater the less total phosphorus is discharged.

The modelling flow is divided into two sections, neither of which models any effects of filter strips on flow. Section 1 is the bulk of the filter strip which receives the least amount of surface flow. Section 2 is in the middle of Section 1 and only contains 10% of the filter strip area, yet it is the most heavily loaded part of the filter strip, receiving the majority of the flow, the exact percentage of which is user-defined though it typically ranges between 25-75% of field area, with 50% being the default. (See figure 3.1). In the most concentrated 10%, fully channelized flow can occur. The users specifies what percentage of the flow is fully channelized in this segment, which then does not undergo reduction in pollutants from the filter strip (White and Arnold, 2009).

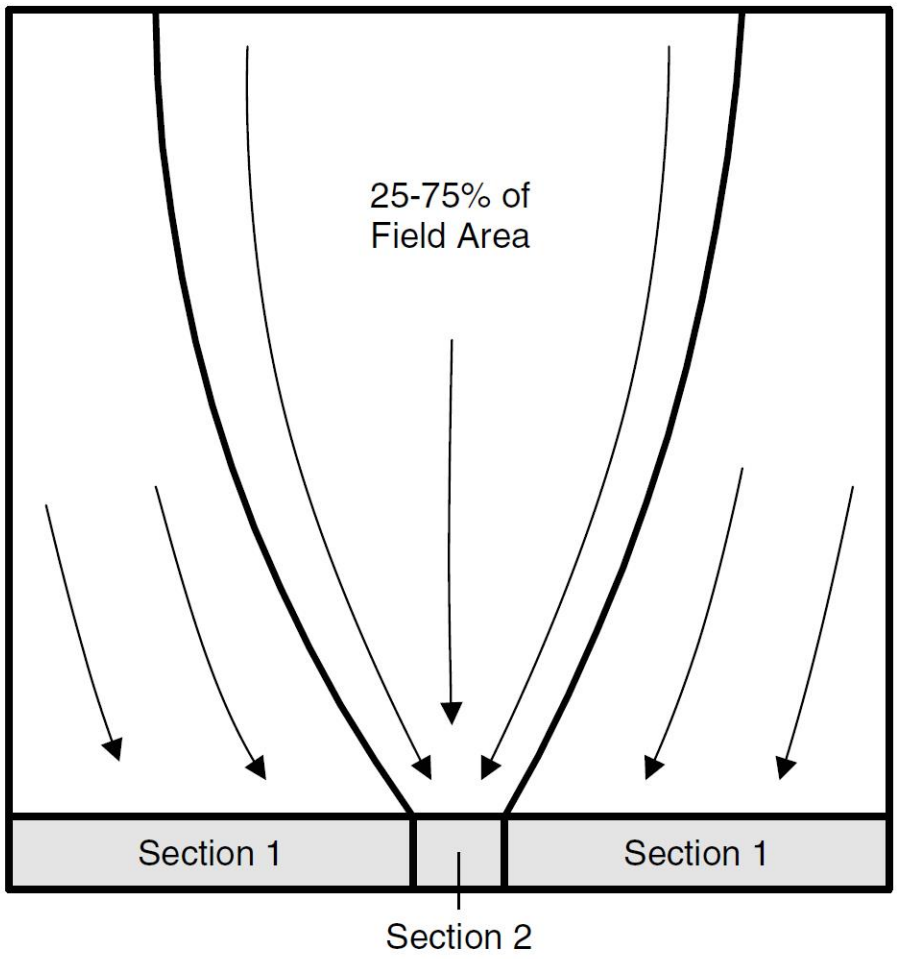

Figure 3.1. Representation of filter strips in SWAT (White and Arnold, 2009).

The SWAT model uses equations based on VFSMOD simulations to calculate reductions in runoff and pollutants (Neitsch et al., 2009). First, the amount of runoff reduction must be known and is found using the equation:

$$R_R = 75.8 - 10.8\ln(R_L) + 25.9\ln(K_{sat}) \qquad (3.52)$$

where R_R is the predicted runoff reduction (%) and R_L is the runoff loading on a given day (mm). Runoff reduction is the most important part of these equations.

Sediment reduction is estimated using the equation:

$$S_R = 79.0 - 1.04 * S_L + 0.213 * R_R \qquad (3.53)$$

where S_R is the predicted sediment load reduction (%) and S_L is the sediment loading (kg/m^2) or the mass of sediment traveling from the upland area (Neitsch et al., 2009).

Since nitrogen and phosphorus pollutants have soluble and sediment-bound particles, the reduction depends on both of these equations. Total nitrogen reduction (%) and nitrate nitrogen reduction (%) can be estimated using the following two equations, respectively:

$$TN_R = 0.036 * S_R^{1.69} \qquad (3.54)$$

$$NN_R = 39.4 + 0.584 * R_R \qquad (3.55)$$

Total phosphorus reduction (%) and soluble phosphorus reduction (%) can be estimated using the following two equations, respectively (Neitsch et al., 2009):

$$TP_R = 0.90 * S_R \qquad (3.56)$$

$$DP_R = 29.3 + 0.51 * R_R \qquad (3.57)$$

3.3.5. Wetlands

Water movement

Since the soil around the Little Vermillion Watershed contains poorly drained soils, much of the initial land cover prior to settlers arriving was wetlands. Wetlands serve important hydrologic, geochemical, and biological functions within the watershed, making wetland restoration a best management practice in this watershed in the reduction of pollutants and mitigation of large amounts of runoff (Wang et al., 2010). The SWAT model treats wetlands as water bodies within a subbasin, which are defined by user input parameters (Neitsch et al., 2009).

In order to calculate precipitation and evaporation from the wetland, the surface area needs to be known. The SWAT model requires the user to input two of the following for surface

area and volume calculations: normal surface area, normal water volume, maximum surface area, and maximum water volume (Arnold et al, 2012a). After inputting two of the parameters, SWAT can then solve for the other two. The SWAT model updates the surface area using the equation (Neitsch et al., 2009):

$$SA = \beta_{sa} * V^{expsa} \qquad (3.58)$$

where SA is the surface area of the wetland (ha), V is the day's volume (m^3 H_20), β_{sa} is a coefficient, and expsa is an exponent.

Both β_{sa} and expsa are functions of normal and maximum conditions, given in the equations:

$$expsa = \frac{\log_{10}(SA_{mx}) - \log_{10}(SA_{norm})}{\log_{10}(V_{mx}) - \log_{10}(V_{norm})} \qquad (3.59)$$

$$\beta_{sa} = \left(\frac{SA_{mx}}{V_{mx}}\right)^{expsa} \qquad (3.60)$$

where the subscripts represent the maximum and normal wetland conditions (Neitsch et al., 2009).

The wetland is assumed to only release water via flow out when the volume is greater than the normal volume. On a given day, if the volume is greater than normal volume, outflow is calculated by the equations (Neitsch et al., 2009):

$$V_{flowout} = \frac{V - V_{norm}}{10} \qquad (3.61.1)$$

$$\text{if } V_{norm} \leq V \leq V_{mx}$$

$$V_{flowout} = V - V_{mx} \qquad (3.61.2)$$

$$\text{if } V \geq V_{mx}$$

Water lost due to seepage is governed by the equation (Neitsch et al., 2009):

$$V_{seep} = 240 * K_{sat} * SA \qquad (3.62)$$

where K_{sat} is the saturated hydraulic conductivity of the bottom of the wetland.

Nutrient movement

When nutrients enter into the wetland, they can either settle out of the water, be used by microorganisms in the wetland, or exit through discharge. The mass (kg) of the nutrient leaving on a given day is calculated using the equation:

$$M_{settling} = v * c * A_s * dt \qquad (3.63)$$

where *v* is apparent settling velocity (user-specified) (m/day) (apparent because it represents the processes that bring in nutrients into the wetland), *c* is the initial concentration of nutrient in the wetland (kg/m^3 H_20), A_s is the area of the sediment-water interface (m^2), and dt is the time step (1 day) (Neitsch et al., 2009).

One of the main purposes of wetlands in reducing the nutrient level is the growth of algae to use the excess nitrogen and phosphorus. The following equation developed by Rast and Lee (1978) calculated the amount of chlorophyll in the wetland relative to the amount of phosphorus:

$$Chla = Chla_{co} * 0.511 * p^{0.76} \qquad (3.64)$$

where Chla is the chlorophyll *a* concentration (µg/L), $Chla_{co}$ is a user-defined parameter that allows for the adjustment in chlorophyll *a* concentration if phosphorus is not the limiting factor in algae growth (default set at 1.00), and *p* is the total phosphorus concentration (µg/L).

The amount of algae is assumed to be proportional to the amount of chlorophyll *a*, represented by the following equation:

$$algae = \frac{chla}{\alpha_o} \qquad (3.65)$$

where algae is the algal biomass concentration (mg algae/L) and α_o is the ratio of chlorophyll *a* to algal biomass (µg chla/mg alg) (Neitsch et al., 2009).

4. Methodology

4.1. Data

4.1.1. Site description

LVR is an approximately 489 km^2 watershed located primarily within Vermillion County, IL, though it stretches into nearby Champaign and Edgar Counties (only 400 km^2 drains into the outlet used for this study) (see Figure 4.1 for a picture of the study watershed) (Algoazany, 2006). It is an agriculturally-dominated watershed with the primary crop rotation of corn and soybeans, with the average annual rainfall in nearby Danville, IL, at 1040 mm. The majority of the watershed has slopes of less than 1%, with the dominant soil series being the associated Drummer silty clay loam and Flanagan silt loam series. With the majority of the watershed being flat and Drummer being a naturally poorly drained soil, man-made tile drainage was required for the conversion of the land into high quality agricultural land. This has led the majority of the hydrology to be altered so that most of the water is drained by tiles into man-made ditches. Watersheds like LVR contribute heavily to the hypoxia zone ecological problem within the Gulf of Mexico. Another problem associated with this watershed has been found with a reservoir located within the watershed that is used by Georgetown, Illinois, for drinking water; this reservoir has tested positive for elevated levels above the MCL for nitrate.

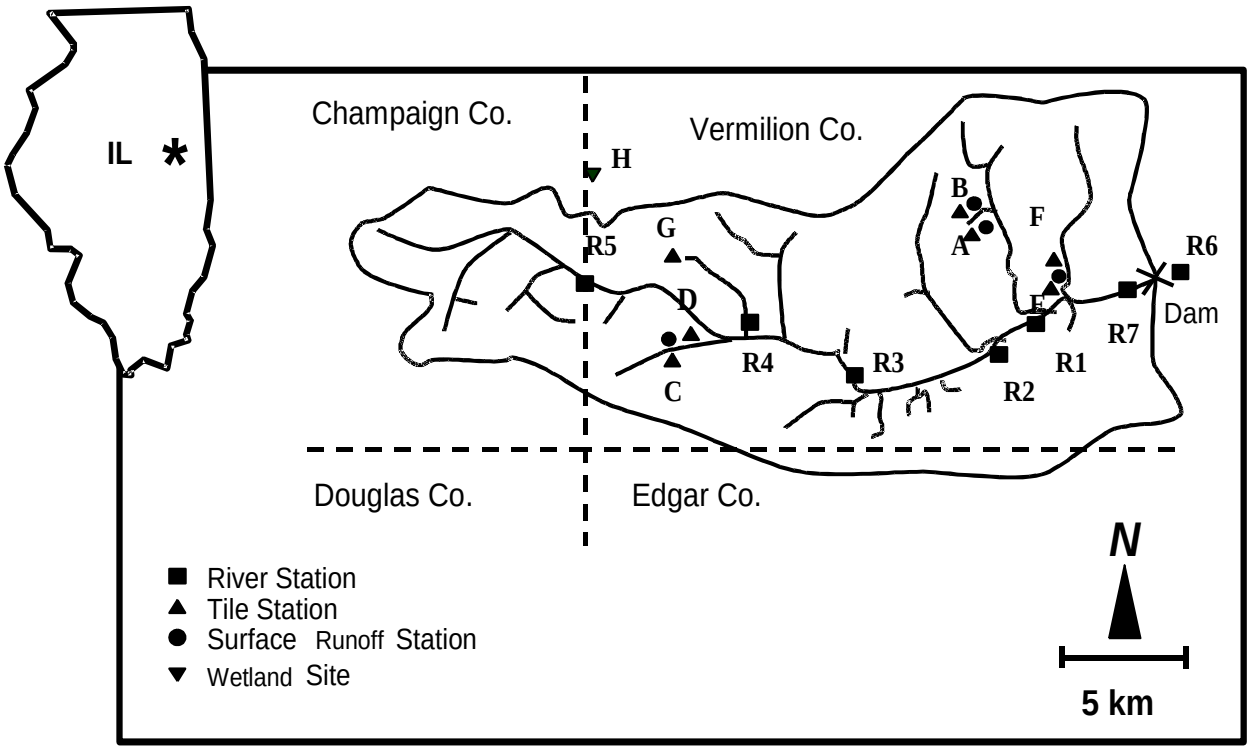

Figure 4.1. Map and Station Location of study watershed

4.1.2. Data collection

The LVR water quality monitoring project was started in 1991 by the University of Illinois as a long-term water quality and flow monitoring project (Algoazany, 2006). Seven subsurface and four surface monitoring stations were created at farms located within the watershed, with three river stations located at various distances from the river source. These farms also provide management operation information. The outlet river station for this model is located west of a dam before LVR crosses into Indiana (R7). The R7 station was started in 1996 and continued through the end of 2000, but there were problems at the beginning of station operation and that were not fixed until mid-1997, which led to only 1998-2000 being used for calibration and validation data.

The station farms located throughout the watershed are considered typical for this area in their management operations. Subsurface drains tend to be 1.0 to 1.1 m deep (Algoazany, 2006).

All farm monitoring stations had a corn-soybean rotation, the majority using conservative tillage practices. For fertilizer application, ammonia was generally placed before corn planting, and a low-nitrogen with phosphorus fertilizer was used after the soybean harvest, typically followed by tillage operation.

The river monitoring stations each had daily stage gauge readings recorded, though the readings tended to be more frequent after large storm events (Algoazany, 2006). At each reading, a water-quality sample would be taken for analysis at the Water Quality lab in Urbana, Illinois.

Until an analysis could be done, collected samples were preserved with concentrated sulfuric acid (2 ml L^{-1}) and stored at 4 ^{o}C (Algoazany, 2006). After adding a solution of hydrazine sulfate containing a copper catalyst in order to reduce nitrate to nitrite, a treatment of sulfanilamide then causes the nitrites to form azo dye, which was measured colorimetrically at 520 nm. The result measures the combined nitrate and nitrite concentration in solution, though the test fails if the nitrite concentration after the first step is not greater than 0.07 mg L^{-1}.

In order to determine the amount of phosphate in the sample, the solution was treated with molydate and antimony ions, which causes the solution to form a blue color (Algoazany, 2006). The solution was then reduced by an acidic solution of ascorbic acid. A colorimetrical analysis measures the amount of light absorbed at 660 nm in order to determine the amount of soluble phosphate in the solution. The test cannot detect phosphate if the amount in solution is less than 0.1 μg L^{-1}.

Measured data analysis

River flow tends to follow the precipitation patterns before the plants are fully established (see Figure 4.2). The growing season starts at planting in April, with the plants not being fully

established until July; heavy rainfall during the start of the growing season leads to the heavy usage of tiles for water discharge. After the crop is fully established, the evapotranspiration demands cause the river level to be low until after harvest, when crops are no longer on the field. With the soil frozen during the winter, surface runoff tends to contribute most to any peak events prior to the beginning of the growing season because the tiles during the winter months. During the middle of January, there was warmer weather and a large storm event that caused higher than normal discharges from the fields. Comparatively, 2000 was the driest year of the observed period.

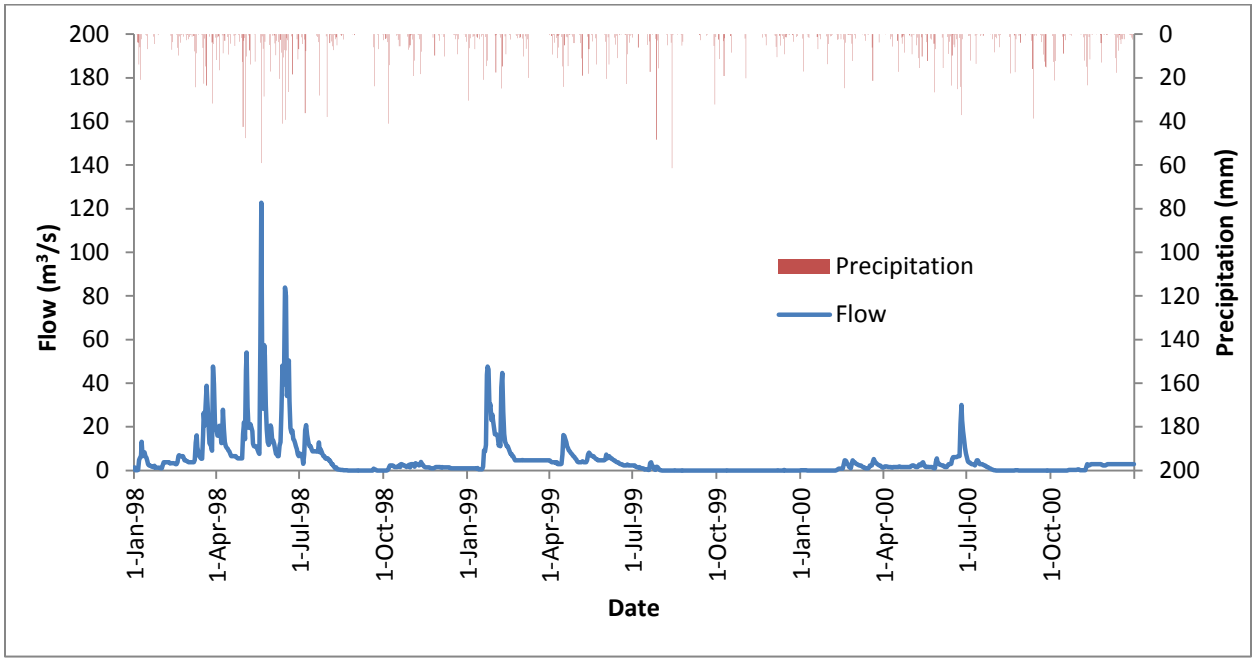

Figure 4.2. Observed flow and precipitation flow pattern in watershed (1998-2000, daily)

At the beginning of the growing season, most corn crops are fertilized with ammonia. The heavy rainfall prior to July when the crops become fully established leads to large amounts of nitrate exiting the soil matrix via tile drainage. Freshly applied fertilizer is more susceptible to nutrient loss because it has not yet been incorporated into the soil matrix. With little biological activity occurring in mid-winter, the large storm events starting in mid-January 1999 resulted in

large amounts of nitrate discharge (see Figure 4.3). The following year the soil held on more tightly to the nitrate supply than in the year previous.

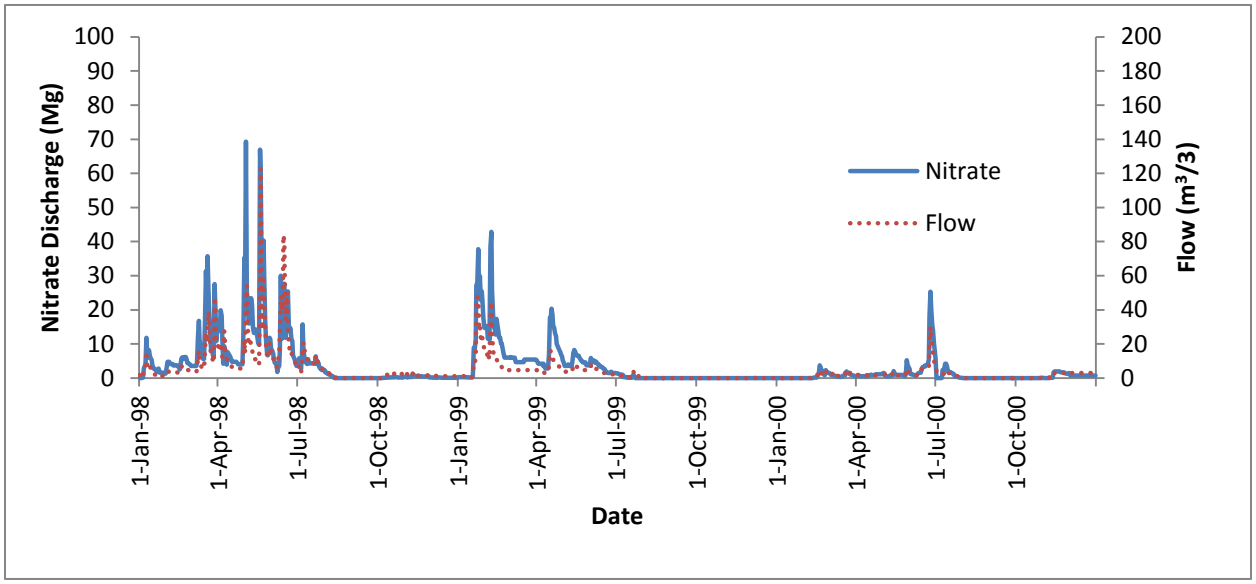

Figure 4.3. Observed Nitrate and Flow pattern at watershed outlet (1998-2000, daily)

Concentration tends to also follow the seasonal pattern of peaking in May/June, when the crops are in the develop stage (see Figure 4.4). Concentration tends to be above the MCL after spring fertilization until the crops reach the midseason growth stage. Once the flow begins to subside in July, the concentration drops below MCL levels. Without crops on the field to utilize nitrogen during the peak event in 1999, more nitrogen was available for discharge, leading to higher concentrations. Since nitrate discharge and flow were both low in 2000, concentration rarely went above 10 ppm as well as the fact that the peak storm event for the year does not occur until after midseason growth stage.

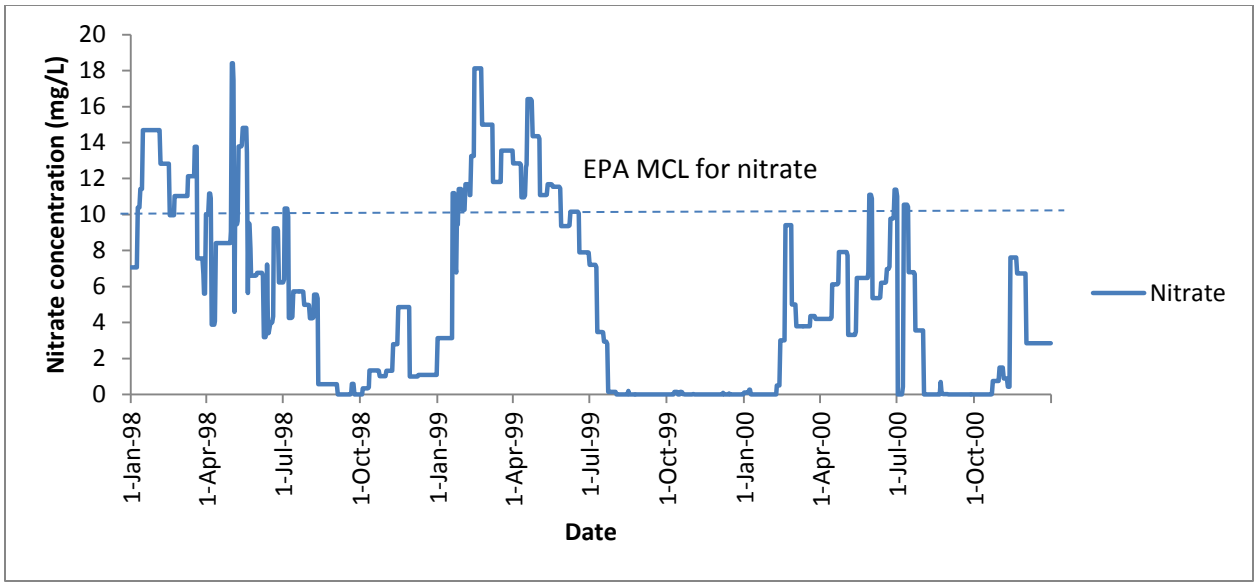

Figure 4.4. Nitrate concentration and flow at watershed outlet (1998-2000, daily)

Phosphorus discharge follows the same seasonal patterns as nitrate discharge (see Figure 4.5). Because phosphate is less soluble and less plentiful in the soil and fertilizer application than nitrates, the magnitude of phosphate discharge from the soil is much smaller, and phosphorus discharge tends to occur mainly in the storm events and not in baseflow. The late January/earlier February 1999 storm event flushed out much of the soluble phosphate in the soil, leaving less for when the growing season flow peak occurs.

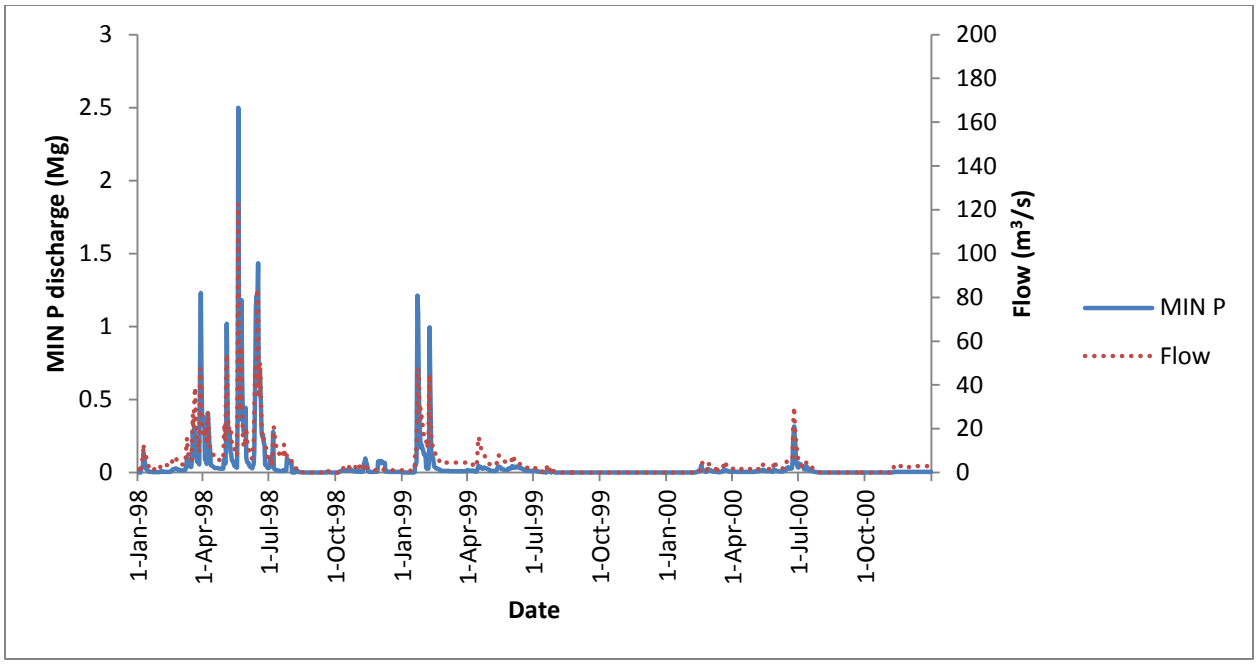

Figure 4.5. Daily MIN P discharge and flow at watershed outlet (1998-2000)

Phosphorus concentration tends to lag the flow for the growing season peak (see figure 4.6). The growing season peak discharge makes the conditions more favorable for phosphorus to become soluble. Also, another peak in concentration occurs after fall fertilization. Since the fertilizer placed after soybean harvest has yet to incorporate into the soil matrix, water discharge can more easily pick up the phosphorus.

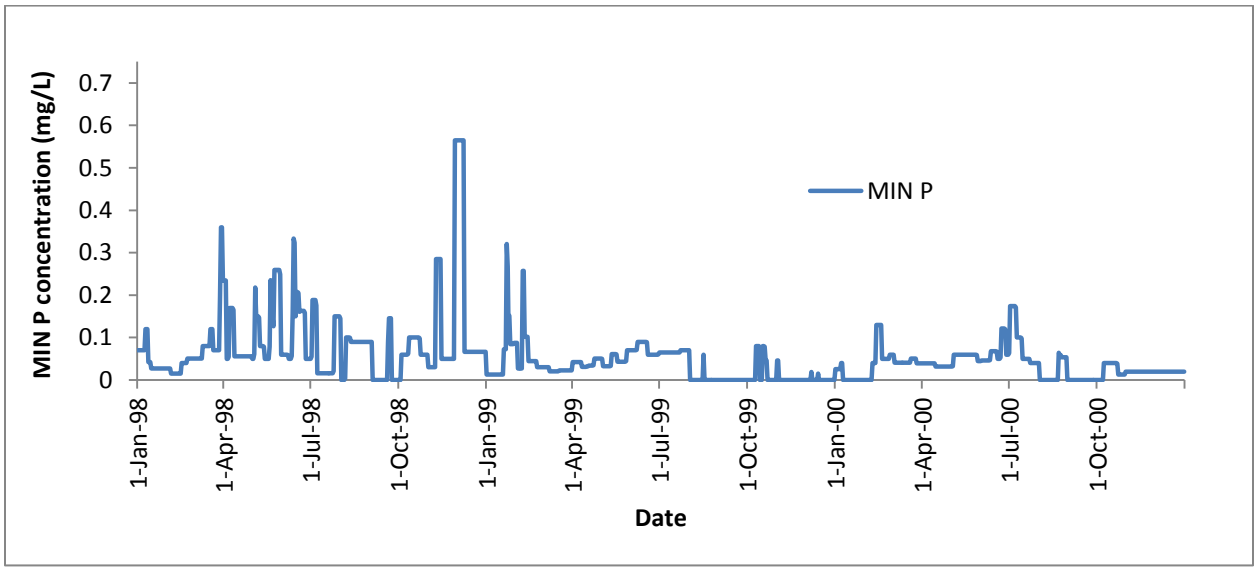

Figure 4.6. Daily MIN P concentration at watershed outlet (1998-2000)

Analyzing this data has revealed certain problems. The river station had problems with the weir from 1996-mid 1997 and no data beyond the year 2000, leaving only 3 complete years available for analysis. Soil sediment was not included in the analysis because it was not constantly measured at the river station. Some days had extrapolated data from the previous measurement as the input.

4.1.3. Input data for SWAT

This study uses ArcSWAT 2012 extension for ArcGIS 10.1. Data sets were re-projected into the NAD 1983 UTM Zone 16N projection for more accurate measurements.

Most of the input data needed for SWAT can be obtained from internet sources. A 10x10 meter resolution Digital Elevation Model (DEM) and National Land Cover Data (NLCD) 2006 were obtained from the USGS seamless survey (http://viewer.nationalmap.gov/viewer/). The SWAT model uses the DEM data to determine the direction and accumulation of water flow (Winchell et al., 2010).

The SWAT model HRUs require additional data about land cover and the soils. The NLCD data provides some basic information about land usage, but agricultural land is defined generically. Srinivasan et al. (2010) used Cropland Data Layers (CDL) from the USDA National Agricultural Statistics Survey in combination with NLCD data (http://nassgeodata.gmu.edu/CropScape/). As a supplement to 2006 NLCD data, 1999-2003 Cropland Data was used to create a 4 year crop rotation for the agricultural land. After obtaining and projecting CDL data for 1999-2003, a majority filter (number of neighbors 4, replacement threshold, half) was done in an attempt to remove noise. Before combining the CDL layers to determine crop rotations, values were reclassified to assume anything that was not corn or

soybeans to be insignificant (Raster value zero). To combine the data layers, the raster calculator used the equation CDL 1999*1000+CDL 2000*100+CDL 2001*10+CDL 2002*1 in order to determine the rotation. If at least three years were not planted as corn or soybeans, it was assumed that CDL 1999 data held throughout the period. Before combining the new raster with the CDL data, another reclassification was done, with the corn-soybean rotation being noted (Corn-Soybean is corn planted odd year and soybean planted even year, with the reverse being true for Soybean-Corn). Another raster calculator operation replaced agricultural data in the NLCD data with CDL data. A custom look table needed to be created for this new data set, combining the NLCD lookup table with the CDL rotation table (see Figure 4.7 for land use across LVR) (see Appendix A Table A-1 for more detailed land use information).

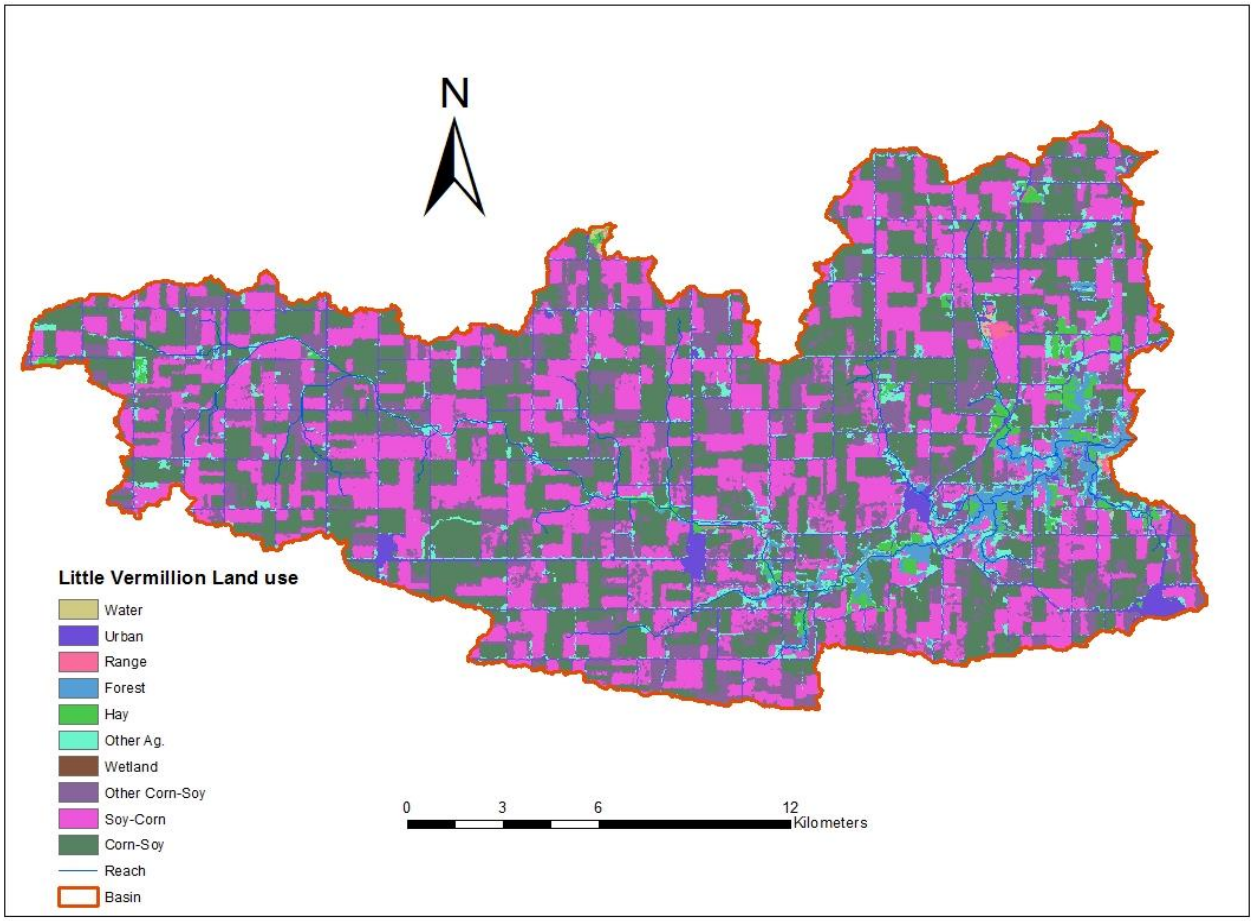

Figure 4.7. LVR Land Use distribution

Soil data for the Illinois counties of Champaign, Edgar, and Vermillion can be obtained from the Soil Survey Geographic Database (SSURGO). (See Figure 4.8 for soil distribution across watershed, See Appendix A Table A-2 for detailed soil data).

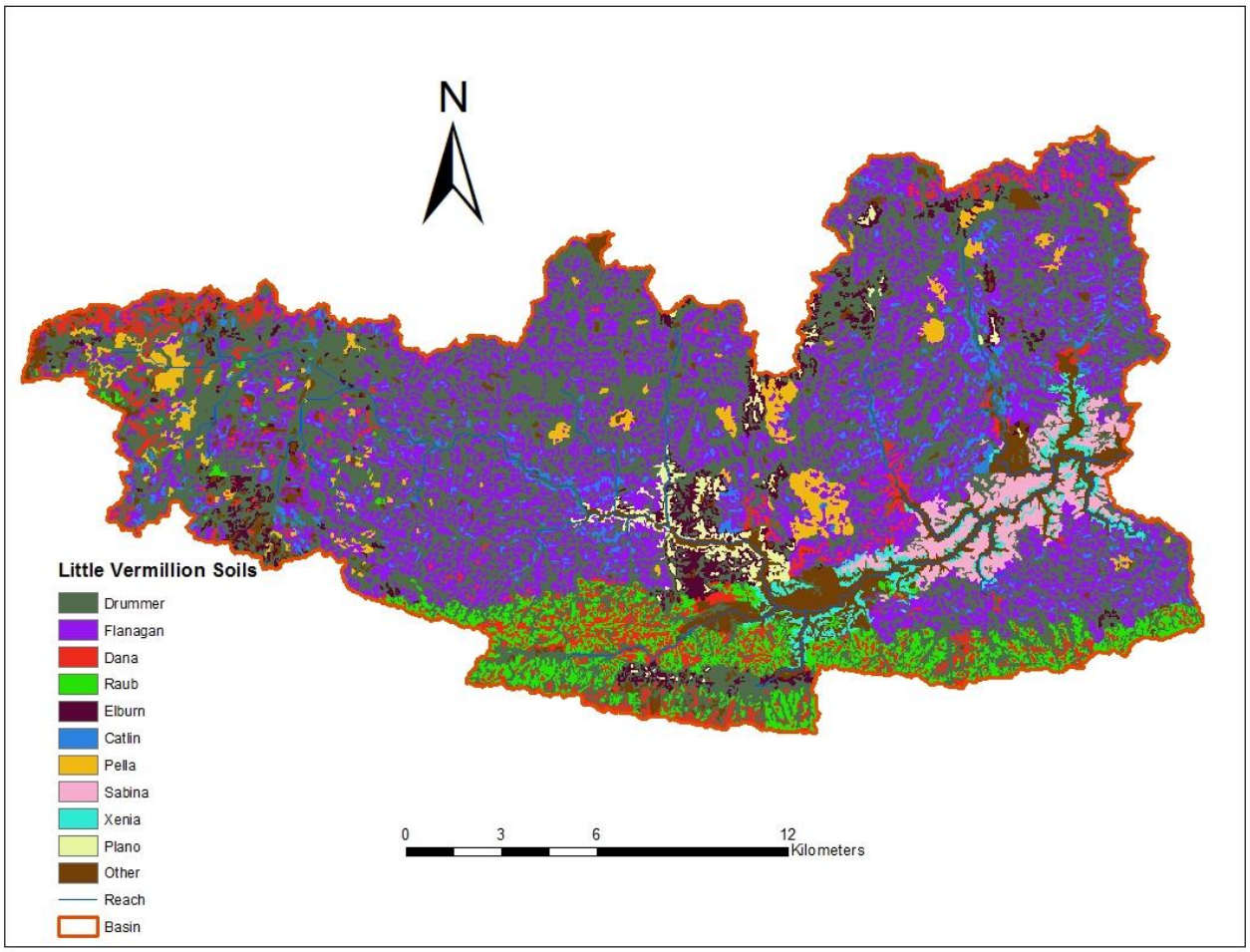

Figure 4.8. LVR soil series distribution

The USDA Agricultural Research Service (ARS) provides daily temperature and precipitation on a county wide basis from 1950 to 2010, which is available online. Data sets for Champaign, Vermillion, and Edgar counties were obtained and combined into temperature and precipitation lookup tables. The other weather data sets (weather generator, relative humidity, solar radiation, and wind speed) can either be derived from observed data sets or simulated. This

study used the WGEN_US_COOP_ 1960_2010 monthly weather database and let SWAT create simulated tables for relative humidity, solar radiation and wind speed.

4.2. SWAT setup

4.2.1. Calibration and validation

Before SWAT delineates streams and outlets, SWAT requires an area of flow accumulation in hectares (ha). The SWAT model can then delineate the main channel, tributaries, and outlets. The SWAT model defines the boundaries of the study area by the chosen outlet of which to define the watershed. For this study, flow accumulation area was 388 ha, and an outlet was manually added in order for the defined watershed's area to be approximately 98,725 acres. The number of subbasins created was 37, with a total basin drainage area of 98,390.3 acres (see Figure 4.9 for the delineated watershed).

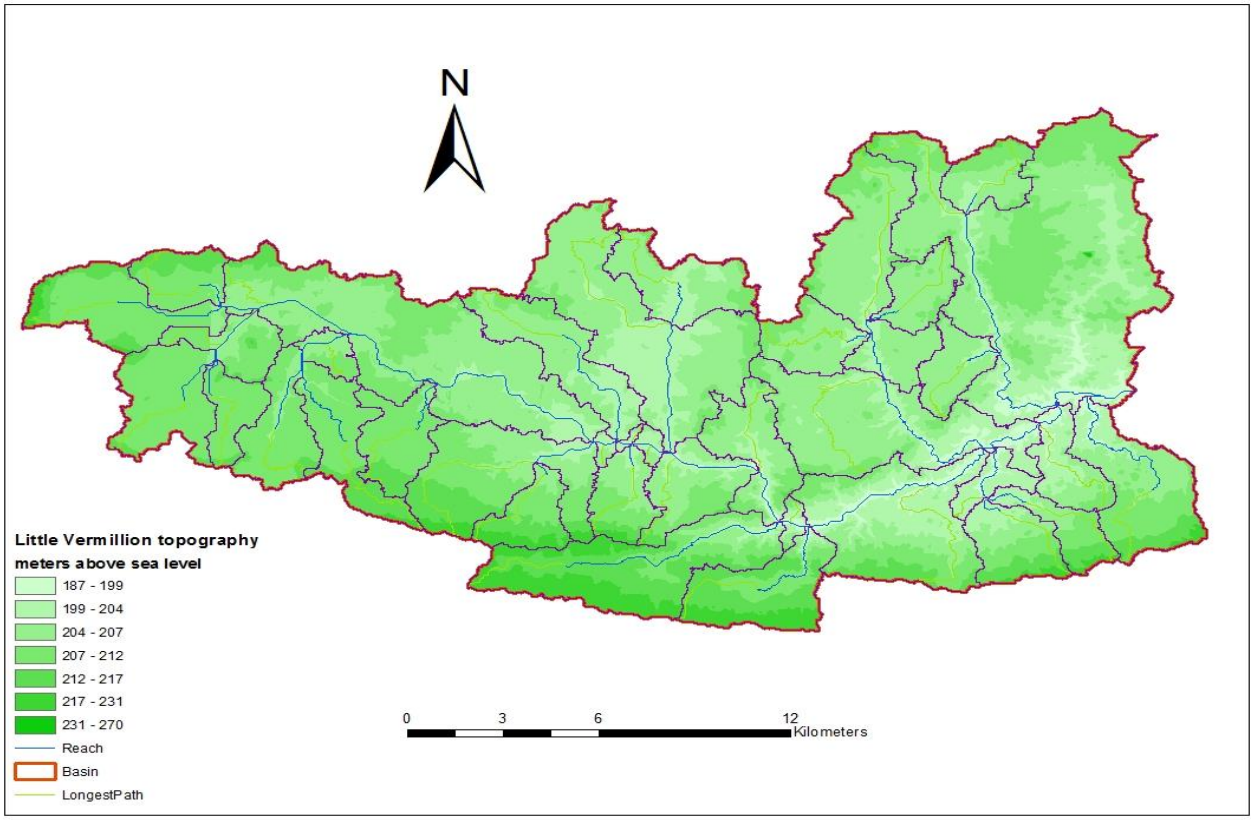

Figure 4.9. LVR DEM and subbasins

Before HRUs could be classified, the DEM had to be separated into different slope classes. The mean slope for the watershed was 1.1%, but the maximum slope was 109%. This study used three slope classes, with the upper limits of the slope classes being 1%, 5% and 109% (see Figure 4.10 for slope class distribution). After land cover, soil data and slope classes were added to the project, a threshold percentage was needed to be defined in order to remove statistical insignificant land covers, soils, and slope classes. A land cover type had to cover 15% of a subbasin, while a soil had to cover 10% of the land cover and slope had to encompass 35% of the soil, with an exception to urban land and water. 417 HRUs were created using this definition. (See Appendix A Tables A-1 and A-2 for land use and soil percentages, respectively, for before and after HRU delineation).

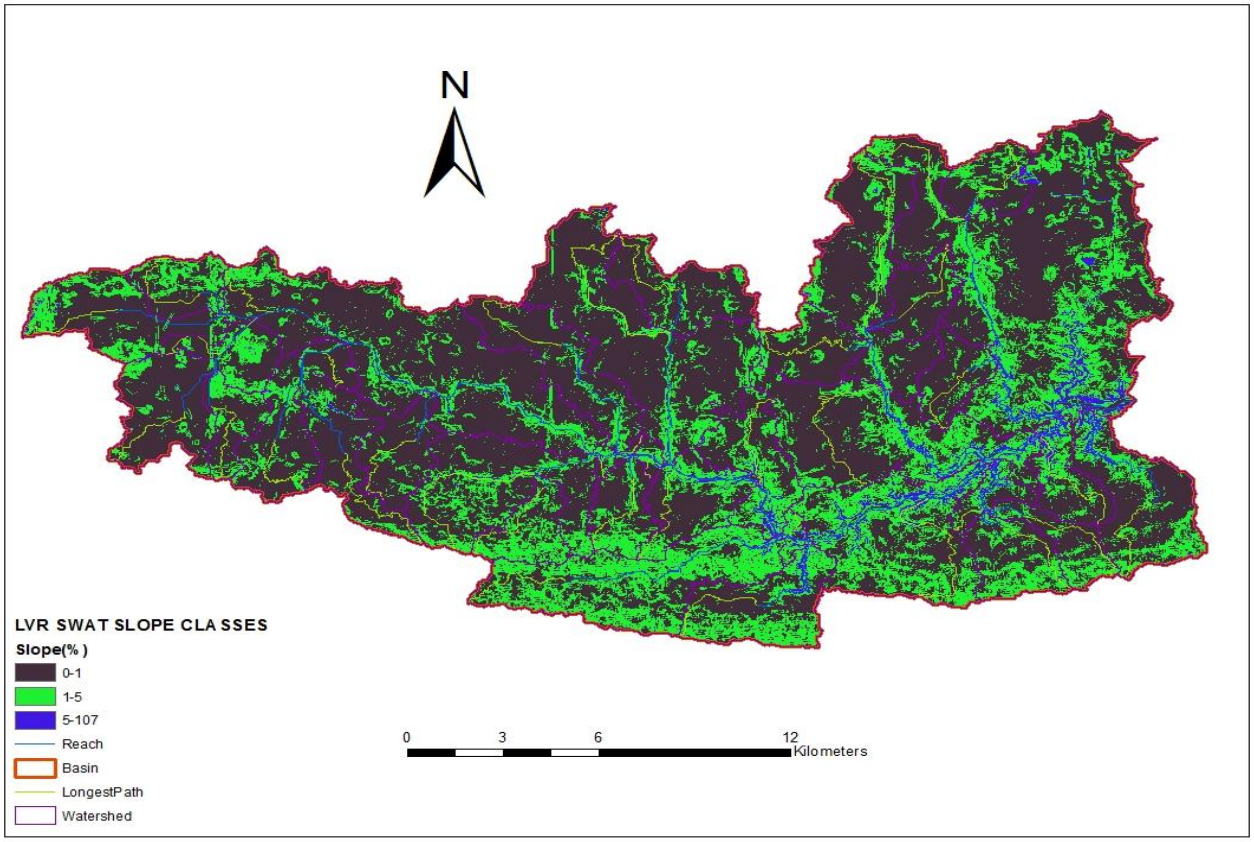

Figure 4.10. LVR SWAT slope classes

After the weather data definition was complete, information regarding agricultural practices needed to be entered into the model. Since the agricultural area in the watershed is artificially drained via tiles, subsurface drainage tiles were implemented at 1 m depth and 28 m apart with time to drain to field capacity at 24 hrs and a drainage lag time at 48 hrs for agricultural area. The crop rotation management operations for the agricultural lands were derived from stations in the watershed for the period from 1995 to 2000. (See Appendix B.1 for assumed management operations). The tillage operations were assumed to be conventional tillage for the agricultural area.

After SWAT files were rewritten to include changes to management operations, the model was run for years 1998-2000 (which have data), with an initialization period from 1995-1997. The automatic calibration program SWAT-CUP was run using the SUFI routines. Ten

SWAT-CUP simulations were run for each parameter modified. Parameters chosen to modify were based on a review by Arnold et al. (2012b). A rank sensitivity test was performed for all parameters for flow, nitrate (NO_3), and mineral phosphorus (Min P) to determine the sensitivity of the different parameters. All 3 variables were calibrated simultaneously using SWAT-CUP. First, a run using 1998-1999 flow data and 1998 nutrient discharge data was run in order to reduce the range of the most sensitive parameters, with a higher weight placed on the nutrient data. After reducing the range of the most sensitive parameters, the calibration run was done using 1998-1999 flow data and 1998-1999 nutrient data. The best parameters were approximated, and then the model was run for 2000 data.

Nash-Sutcliffe coefficient was used as the calibration reference to determine the best parameters. Nash-Sutcliffe (NS) coefficient is commonly used goodness of fit measure for hydrologic and water quality models. The closer the NS value is to 1, the more the simulated values correlate with the observed data. The NS value can be computed with the equation (Nash and Sutcliffe, 1970):

$$E_f = 1 - \frac{\sum_{i=1}^{n}\left(\hat{Y}_i - Y_i\right)^2}{\sum_{i=1}^{n}\left(Y_i - \bar{Y}\right)^2} \quad (4.1)$$

where E_f is the efficiency index or NS, $\hat{Y}_i$ and Y_i are the predicted and measured values of the dependent variable Y, $\bar{Y}$ is the mean of the measured values, and n is the sample size.

Another statistic used to determine calibration is percent bias. Percent bias (PBIAS) measures the percent deviation of the simulated data compared to the observed data (Moriasi et al, 2007). The PBIAS value can be either positive or negative, with a positive value indicating an underestimation and a negative value indicating an overestimation of the model. On a

monthly basis, the absolute value of PBIAS should be less than 25% for flow and 70% for nutrients. The equation for calculating PBIAS is as follows,:

$$E_f = \frac{\sum_{i=1}^{n} Y_i - \hat{Y}_i}{\sum_{i=1}^{n} Y_i} \quad (4.2)$$

4.2.2. BMPs implementation

Common BMPs evaluated in this study for effectiveness in reducing nitrates and mineral phosphorus were reduced tillage operations, filter strips, and wetlands.

Tillage is a common land management operation used to loosen the soil for planting as well as to mix the fertilizer into the soil (See Appendix B.2 and B.3 for reduced tillage and no tillage management operations, respectively). By reducing tillage, the soil is less disturbed and will be less able to erode the soil and the nutrients within. Field station data from within the watershed was used to derive the management practices for reduced and no tillage scenarios.

Filter strips are another commonly used practice in order to reduce pollution. Filter strips are placed in the .ops input files. Filter strips are assumed to have been installed prior to the printed simulation period. The SWAT model requires a unitless ratio between the HRU and filter strip areas (Arnold et al., 2012a). Common ratios range from 30-60, with 40 being the default value. Ratios tested are 20, 40, 60, and 80.

Wetlands are included in the .pnd input files. The information on surface area and volume were obtained by a field study by Miller (1999) located near LVR. The SWAT Input/Output documentation suggests the settling rate for nitrogen and phosphorus in the Midwest is 12.7 m/year (Arnold et al., 2012a). Different wetland scenarios tested were 0.2% of subbasin normal surface area 32 cm volume, 0.4% of subbasin normal surface area 16 cm

volume, 0.4% of subbasin normal surface area 32 cm volume, and 0.2% of subbasin normal surface area 64 cm volume.

To determine statistical significance of each BMP, statistical tests were done on both an annual basis. For the annual basis, 1980-2009 were simulated, allowing for a wide variety of precipitation years to be simulated. The statistical test done was a paired Wilcoxon (in R). Additionally, the best tillage practice was combined with the best scenarios of filter strips and wetlands to determine the effectiveness of having multiple BMPs on nutrient pollutant reduction.

5. Results and Discussion

5.1. Calibration and Validation

5.1.1. Calibrated model performance

In order to calibrate the model, parameters had to be changed so that the NS would meet the goal value for the calibration period (see table 5.1 for parameter changes). The uncalibrated daily NS for the calibration period were 0.46 for flow and 0.25 for nitrates, while the validation period NS values were -1.2 for flow and 0.09 for nitrates. The parameters looked at were determined to be the most sensitive based on a review of previous studies done by Arnold et al (2012b). The program SWAT-CUP's SUFI calibration parameter modifies the model parameters for each iteration, and then it determines the best parameters based on NS value. Since SWAT assumes that mineral phosphorus is only discharged via surface runoff, SWAT CUP was not able to obtain calibrated parameters for phosphorus because the watershed hydrology is dominated by subsurface tile drainage.

Table 5.1. Change in parameters for Calibration

Output influenced	Parameter	Parameter description (Arnold et al., 2012a)	Change type	Default	Range	CAL
Flow	CN2.mgt	SCS CN	Relative	1	0.7—1	0.9054
Flow	Sol_AWC.sol	Available soil water content in soil layer (mm H_2O /mm soil)	Relative	1	0.85—1.15	1.0156
Flow	Surlag.bsn	Surface Lag Coefficient	Replace	4	1—5	2.16
Flow	ESCO.bsn	Soil Evap. Comp. Factor	Replace	0.95	0—0.95	0.66
Flow	OV_N.hru	Manning's "n" for overland flow	Replace	0.14	0.14—0.21	0.185
Flow	EPCO.bsn	Plant Uptake Comp. Factor	Replace	1	0—1	0.71

Table 5.1 (cont.)

Flow	GW_REVAP.gw	Groundwater "revap" coeff.	Replace	0.02	0.02—0.2	0.0246
Flow	GW_DELAY.gw	Groundwater delay time (days)	Replace	31	30—50	32
Flow	GWQMN.gw	Min. Depth of Shallow Aquifer for flow to reach (mm H_2O)	Replace	0	0—2	1.37
Flow	REVAPMN.gw	Min. Depth of Shallow Aquifer for percolation to Deep Aquifer (mm H_2O)	Replace	1	1—10	6.38
Flow	CH_N2.rch	Manning's "n" for channel flow	Replace	0.014	0.025—0.065	0.064
Flow	RCHRG_DP.gw	Deep water percolation factor (fraction of percolation from the root zone that recharges the deep water aquifer)	Replace	0	0—1	0.423
Flow	Sol_K.sol	Saturated Hydraulic Conductivity	Relative	1	0.1—10	8.298
Tile Flow	DRAIN_IDEP.ops	Depth to the impermeable layer (set at 1500 mm)	Relative	1	0.8—1.2	1.0175
Tile Flow	DRAIN_T.ops	Time for tiles to drain soil to field capacity (Set at 24 hrs)	Relative	1	1—1.5	1.45

Table 5.1 (cont.)

Tile Flow	DRAIN_D.ops	Depth at which tiles are installed (Set at 1000 mm)	Relative	1	1—1.1	1.1
N	CDN.bsn	Denitrification Exponential Coefficient	Absolute	1.4	0—3	0.002
N	RSDCO.bs	Residue decomposition coefficient	Replace	0.05	0.02—0.06	0.0426
N	N_UPDIS.bsn	Nitrate uptake distribution parameter	Replace	20	15—25	22

Outlet Flow

The SWAT model has a tendency to underestimate the peak flow in the wet year (1998) when compared to the observed data, while non-spring peak flows tend to be overestimated with nonevents sometimes being simulated in the non-growing season (see Figure 5.1). The mass balance comparison (see Figure 5.2) reveals most of the mass difference does not occur from the peak storm events, but from periods following peak storm events. The review of SWAT's new tile drainage equations by Moriasi et al. (2012) found overestimation of monthly peaks. Zhao et al. (2013) also found overestimation for the peaks, but simulated results followed the observed data through the rest of the simulated period. Sahu and Gu (2009) likewise found an overestimation of flow, especially for the wettest year of the study. The SWAT model also has a hard time modelling dry conditions. This could be caused by an incorrect determination of when the conditions are wet, dry, or normal for adjusting the curve number. Another possibility could lie with the curve number method itself. Accuracy is sacrificed for the sake of simplicity in the curve number method. Other methods to measure runoff could be used to improve accuracy for the peak periods of flow.

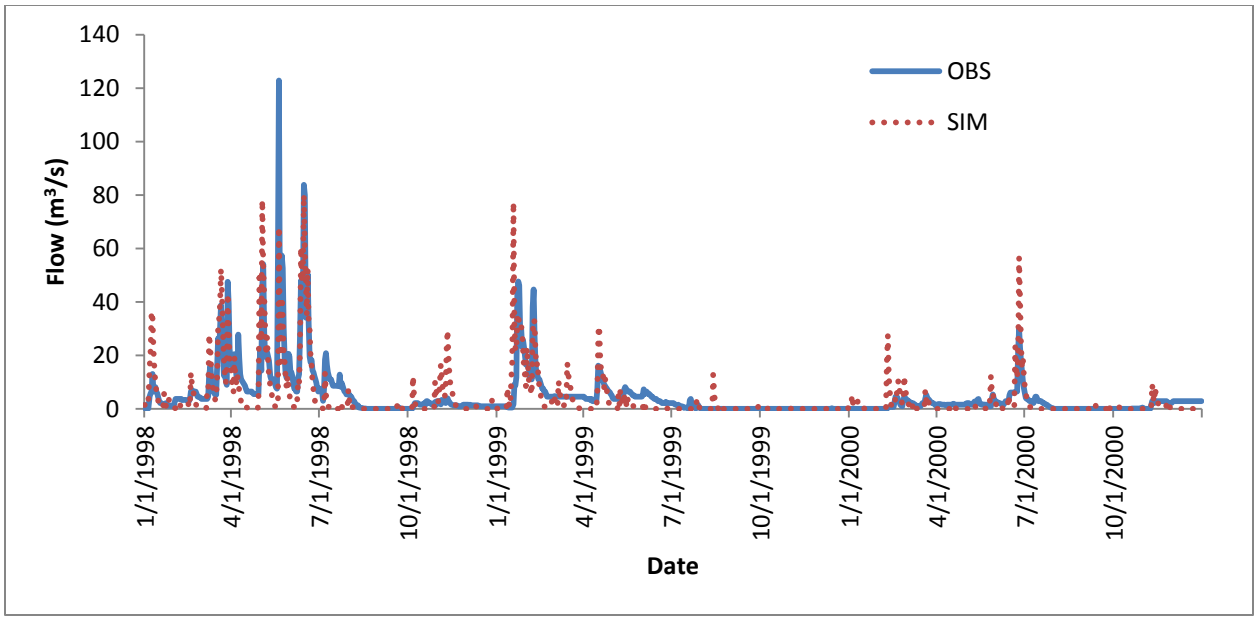

Figure 5.1. Comparison of daily observed and simulated flow at watershed outlet (1998-2000)

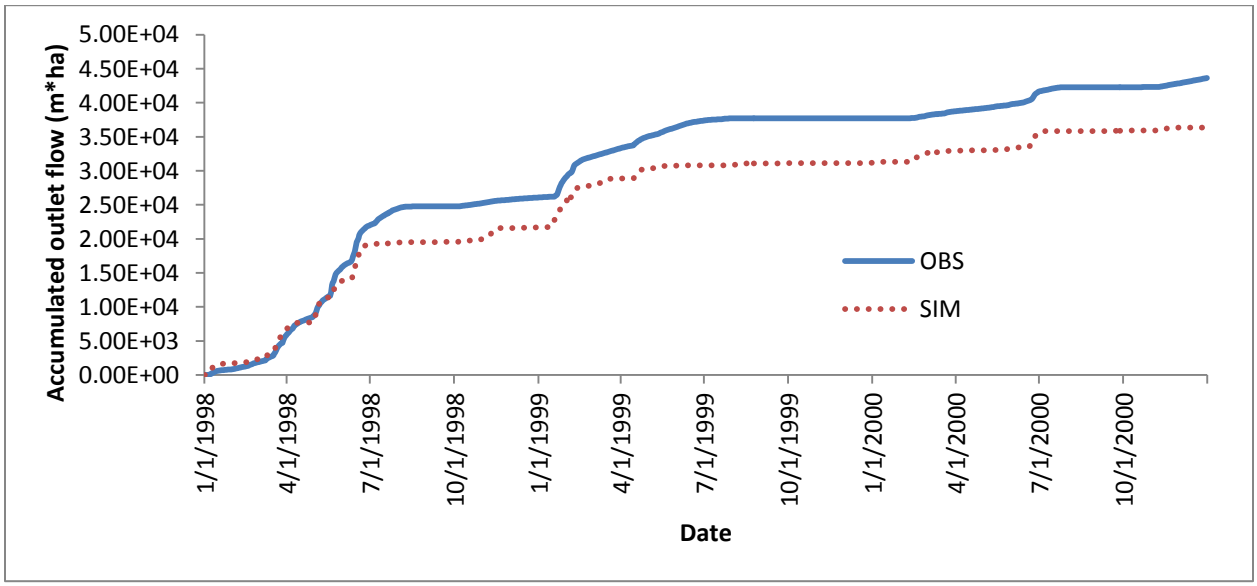

Figure 5.2. Comparison of the observed and simulated flow mass balance at watershed outlet (1998-2000)

One option to consider would be using the Green-Ampt infiltration equation, which is included as an option in SWAT. Green-Ampt requires precipitation data to be in a sub-daily time step. King et al (1999) compared the two methods in a watershed in north central Mississippi. On a monthly basis, the curve number method performed better than Green-Ampt

and was a tighter fit despite underestimations. Ficklin and Zhang (2013) compared the two methods in SWAT uncalibrated on the San Joaquin River watershed in California and found that Green-Ampt was slightly less effective overall but performed better for large storm effects but its effectiveness decreases with increasing watershed size and is not appropriate for simulating watersheds with a lot of saturated areas.

The SWAT model has a tendency to overestimate peaks during the non-growing season and models a quick drop-off in flow. This could indicate a problem in modeling tile flow outside of spring. Despite these difficulties, the calibrated SWAT model has a daily NS value of 0.60 for the calibrated period of 1998-99 and -0.4 for the validation period of 2000. The reason that the validation NS is small is because compared to the other two years, 2000 was a dry year with only one peak event recorded. With much less fluctuation, the small differences have a greater impact on the NS number than in wet years. The percent bias (PBIAS), another calibration statistic, was 17.4% for the validation period and 12% for the calibration period. On a monthly basis, the NS values are 0.83 and 0.3 for calibration and validation periods, respectively, with the calibration and validation PBIAS being 17.3% and 10.7%, respectively. Based on a review done by Moriasi et al (2007), the mode performance rating on a monthly time step based on NS alone would be very good for the calibration period but unsatisfactory for the validation period. Based on PBIAS, the model's results would be Satisfactory for the calibration period and good for the validation period. The program SWAT CUP calculated the sensitivity of the parameters changed using the p-test, which is presented in Table 5.2. Any parameter with a $p>0.1$ was considered to be statistically insignificant.

Table 5.2. Flow parameter Range and Sensitivity Rank

Parameter	Location	Rank
CN2	**.mgt**	**1**
Sol_K	**.sol**	**2**
OV_N	**.hru**	**3**
RCHRG_DP	**.gw**	**4**
Sol_AWC	**.gw**	**5**
SURLAG	**.sol**	**6**

It was suggested by Moriasi et al (2012) that increasing the spacing between drains could help mitigate these errors. The most sensitive tile drainage parameter that they found was drain spacing, with the optimum drain spacing in their study which used an Iowa watershed being 25 m. Sensitivity testing of drain spacing for this model showed no difference when changing drain spacing in the .bsn file because the factors associated with drain spacing are already in the model with the time to drain parameter.

Nitrate Discharge

Like flow, SWAT tends to underestimate the peaks of nitrate discharged (see Figure 5.3 for nitrate discharge and Figure 5.1 for flow). Even when the simulation overestimates the flow peak, nitrate discharge peaks are underestimated. These inaccuracies in peak modelling lead to a large difference in the mass balance between the model and simulated model. These could be due to the inaccurate modeling of pollutants in tile drainage discharge or tile drainage itself. Another possible explanation is the actual non-uniformity of fertilizer application rate and timing could have a greater impact than can be represented in the model. For total nitrogen discharged, Zhao et al. (2013) actually found a tendency of SWAT to overestimate. This could suggest a tendency of SWAT's nitrogen cycle modelling routine to underestimate the transformation of nitrogen from nitrates to other forms.

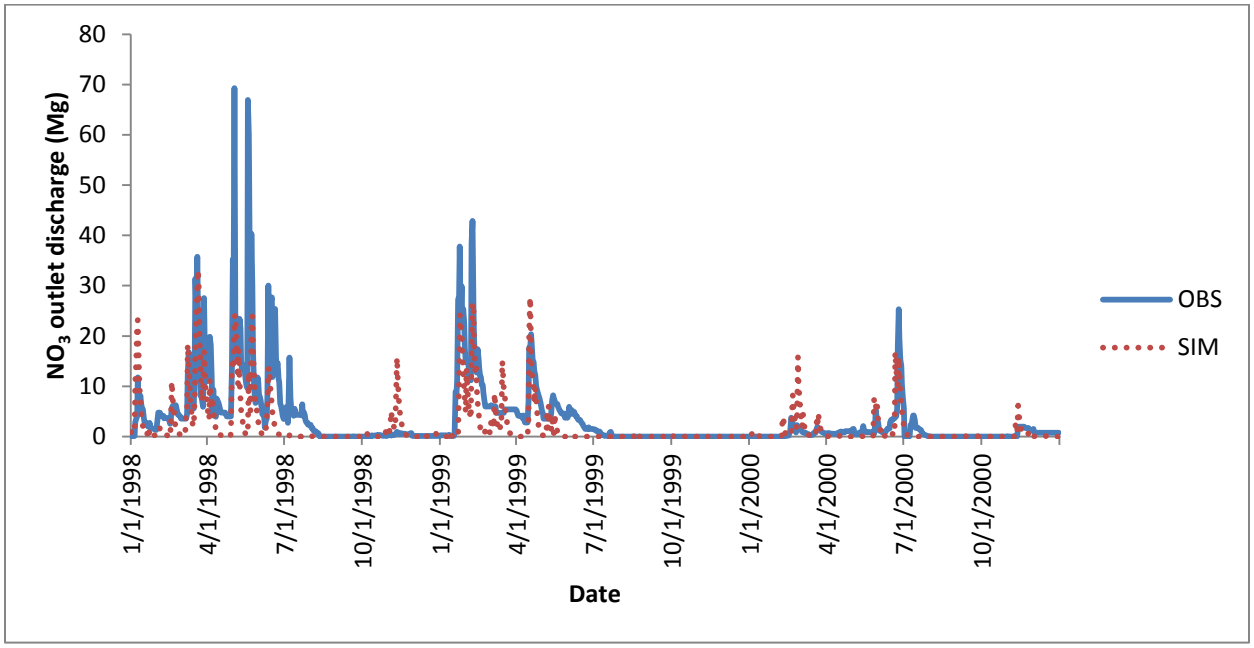

Figure 5.3. Comparison of daily observed and simulated nitrate discharge at watershed outlet (1998-2000)

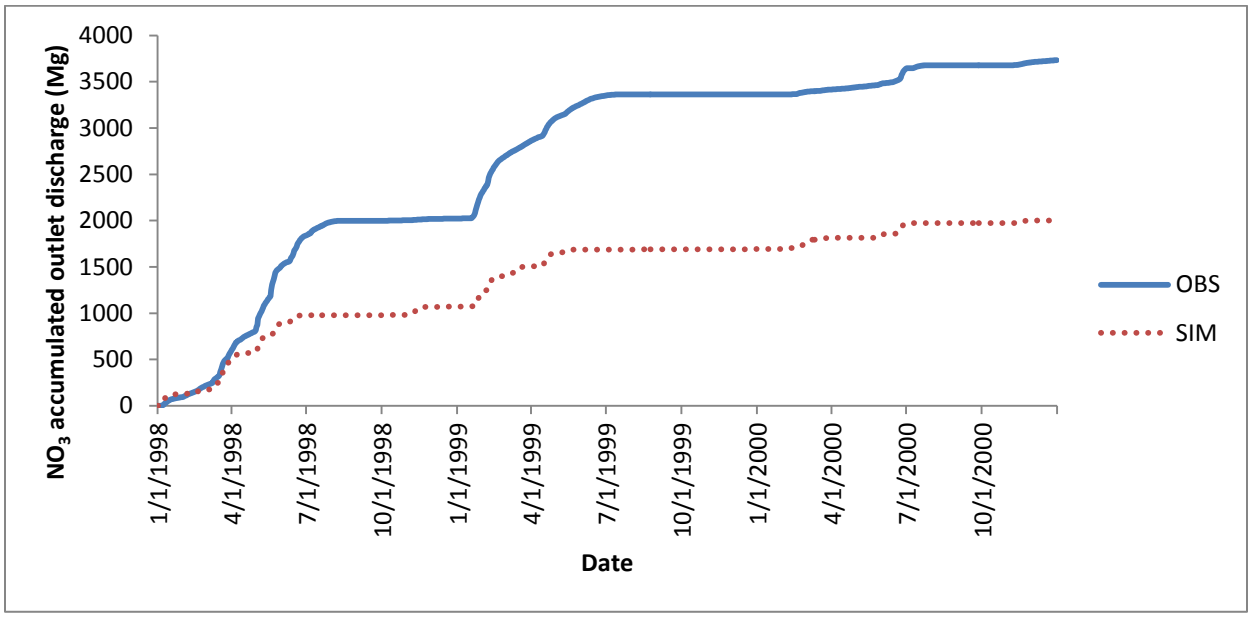

Figure 5.4. Comparison of the observed and simulated nitrate mass balance at watershed outlet (1998-2000)

Using the old tile drainage routines on a comparative study of two tile-drained watersheds in Quebec, Gollamudi et al. (2007) found SWAT continually underestimating the

nitrate load peaks throughout the simulated period on both watersheds. These underestimations were hypothesized to be a result of SWAT's inability to match water yield for those months or small errors in fertilizer load estimation.

However, Sahu and Gu (2009) found the opposite result for their Iowa study. Their un-calibrated model for nitrate discharge found SWAT overestimating the cumulative nitrates at the outlet, with the model having a relatively good NS for nitrates of 0.87. They do mention that, since fertilizer application timing is not spatially uniform, the way the modeler handles that will affect nitrate discharge.

The new tile drainage routines were used in an attempt to more realistically model nitrate discharge in tile flow. Because fertilizer application timing and rate is not actually uniform across the watershed, some amount of user error was introduced in trying to calibrate the model for nitrate discharge. The calibrated model has a daily NS of 0.42 for the calibration period and -0.4 for the validation period, with the calibration and validation PBIAS being 49.7% and 16%, repectively. On a monthly basis, the NS values are 0.5 and 0.67 and the PBIAS valued being 49% and 15.7% for calibration and validation periods, respectively. Based performance ratings given by Moriasi et al (2007), the monthly model would be satisfactory for calibration period and good for the validation period, while ratings based on PBIAS would be satisfactory for calibration period and very good for validation period. The SWAT CUP program's p-test results for sensitivity of parameters for nitrate are presented in Table 5.3.

Table 5.3. Nitrate Parameters sensitivity Rank

Parameter	Location	Rank
CDN	.bsn	1
NPERCO	.bsn	2
ANION_EXCL	.sol	3
RCN	.bsn	4

5.2. BMPs

The Wilcoxon (Wilcoxon, 1945) statistical tests is a common tests used for determining the statistical significance. This test checks on an annual basis what the probability is that the paired columns came from the same source. If the p-value is above 0.05, the BMP was not considered to be statistically significant. Table 5.4 shows the Wilcoxon test for all the BMPs on a yearly basis. All BMPs simulations were found to be statistically significant on a yearly basis for nitrate discharge, while all BMPs except filter strips were also statistically significant for flow.

Table 5.4. Yearly Wilcoxon p-values

BMP	Flow	NO_3
Filter Strips	N/A	1.813e-06
Wetlands	2.194e-06	1.816e-06
Reduced Tillage	0.004979	0.001038
No Tillage	0.0001529	1.863e-09

5.2.1. Tillage

Reduced tillage is one of the most studied BMPs in reducing pollutants. Reduced and no tillage are two common reduced tillage practices (See Appendix B for all tillage management operations). Figure 5.5 shows the impact on outlet flow by changing from conventional tillage to reduced tillage and no tillage operations. No tillage shows an increase in flow, while reduced tillage shows little change to flow. Figure 5.6 shows that the increase in flow is correlated with increased tile drainage. Tan et al (1998) reports that long term no tillage results in greater preferential flow as a result of increased earthworm population as well as possible improved pore continuity. The SWAT simulation of Lake Erie by Bosch et al (2013) found little impact to total flow by no tillage practices. Tillage removes larger pores when disturbing the soil in order to make planting easy or mix in fertilizer into the soil. Reducing tillage will reduce these disruptions but not eliminate them. This improved drainage allows for tiles to be more efficient during dry years and drain the field to field capacity more effectively. However, field data from Francesconi et al (2014) showed little difference in annual tile between reduced and no-till field plots.

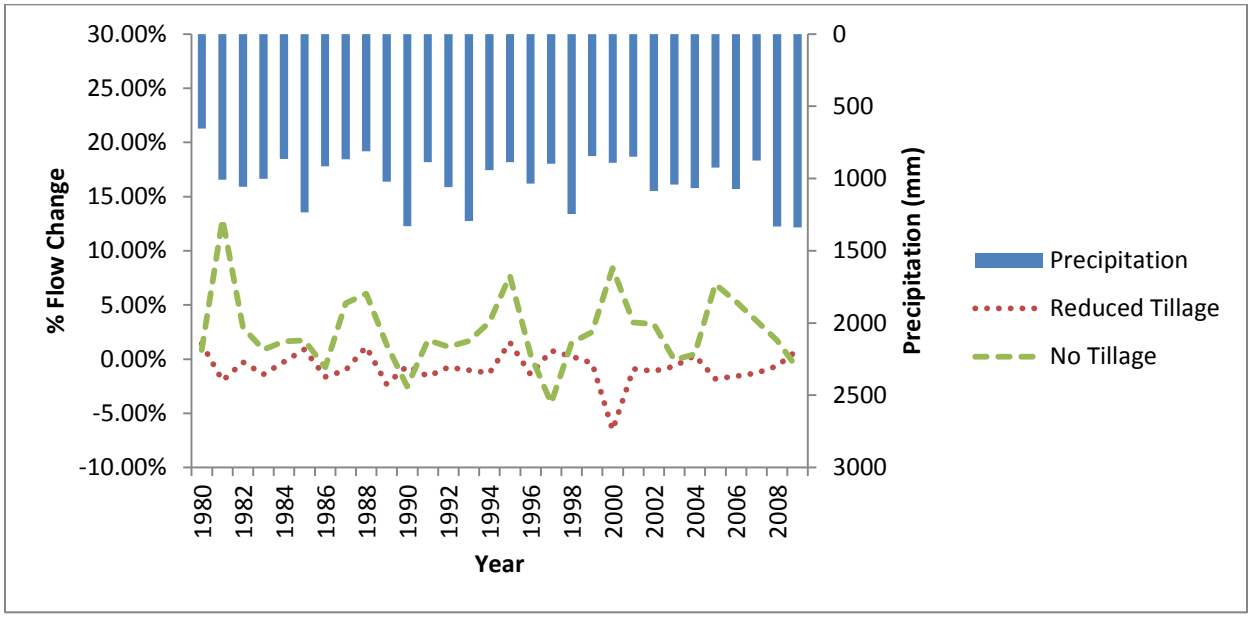

Figure 5.5. Change in outlet for different tillage practices compared to conventional tillage on annual basis (1980-2009)

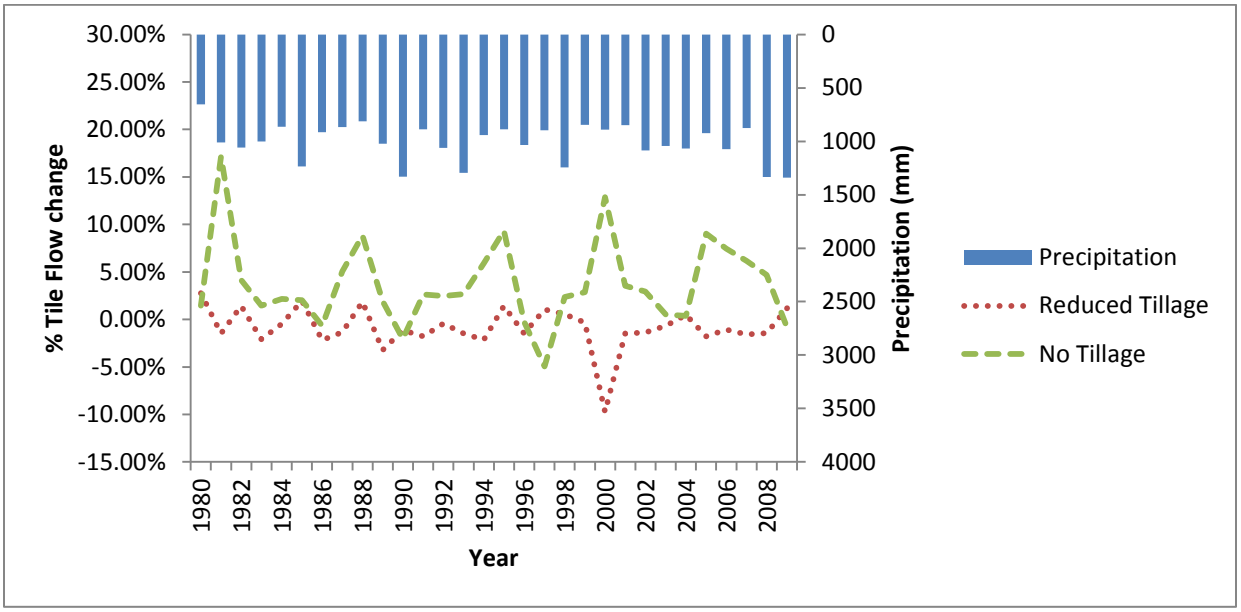

Figure 5.6. Changes in watershed tile flow for different tillage practices compared to conventional tillage on annual basis (1980-2009).

Figure 5.7 shows no tillage reduces the amount of nitrates discharged from the watershed, while Figure 5.8 shows a reduction in nitrate discharged from the tiles under no till. Since tillage helps distribute fertilizer throughout the root zone of the soil profile, nitrate discharge through tiles is also reduced because the fertilizer has to transverse more of the soil profile in order to enter the tiles. Improved aeration by increased earthworm activity helps the root to access more macro pores, which are reconfigured by tillage practices. These observations suggest that no tillage may improve crop nitrogen utilization, but it may also indicate more volatilization. Tan et al (1998) found opposite results in their field study, where the no till plots had more nitrate discharged than the conventional tillage plots in tile flow. Chung et al (2002) found similar results to SWAT's simulated data in that nitrate discharge by no tillage management practices was reduced in a soybean-corn rotation when compared with conventional tillage. The study by Bosch et al (2013) showed little impact of a no-till system on nitrate discharge. Compared with

reduced tillage, Francesconi et al (2014) found in field studies a significant reduction in nitrates discharge in no tillage practices compared to reduced tillage.

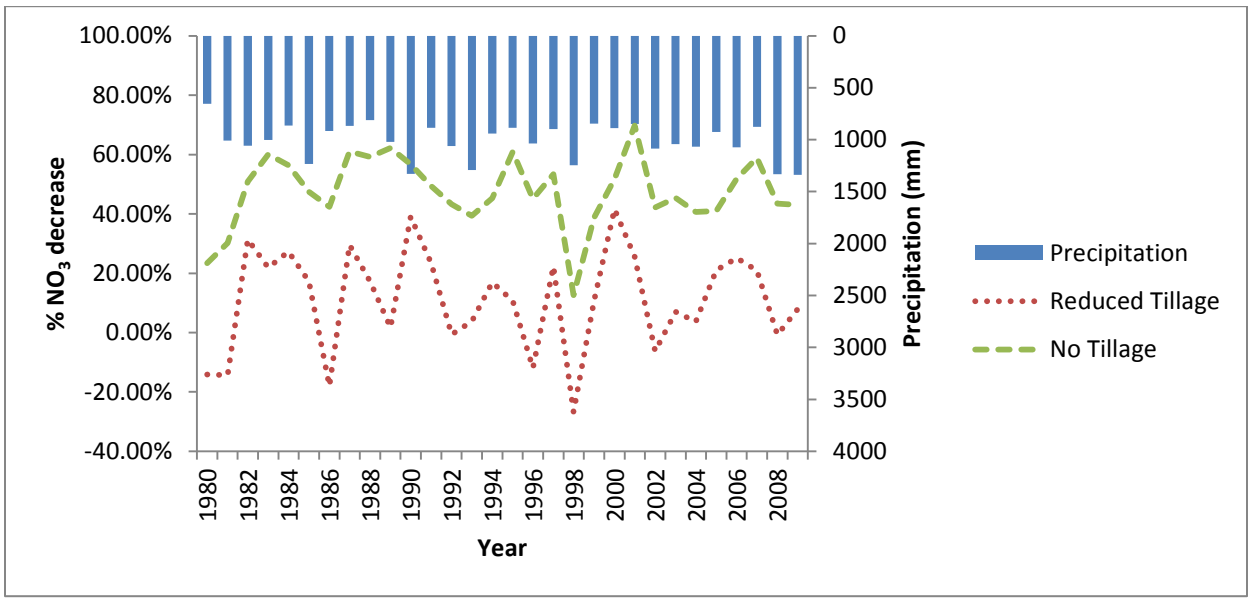

Figure 5.7. Nitrate load reduction in outlet flow for different tillage practices compared to conventional tillage on annual basis (1980-2009).

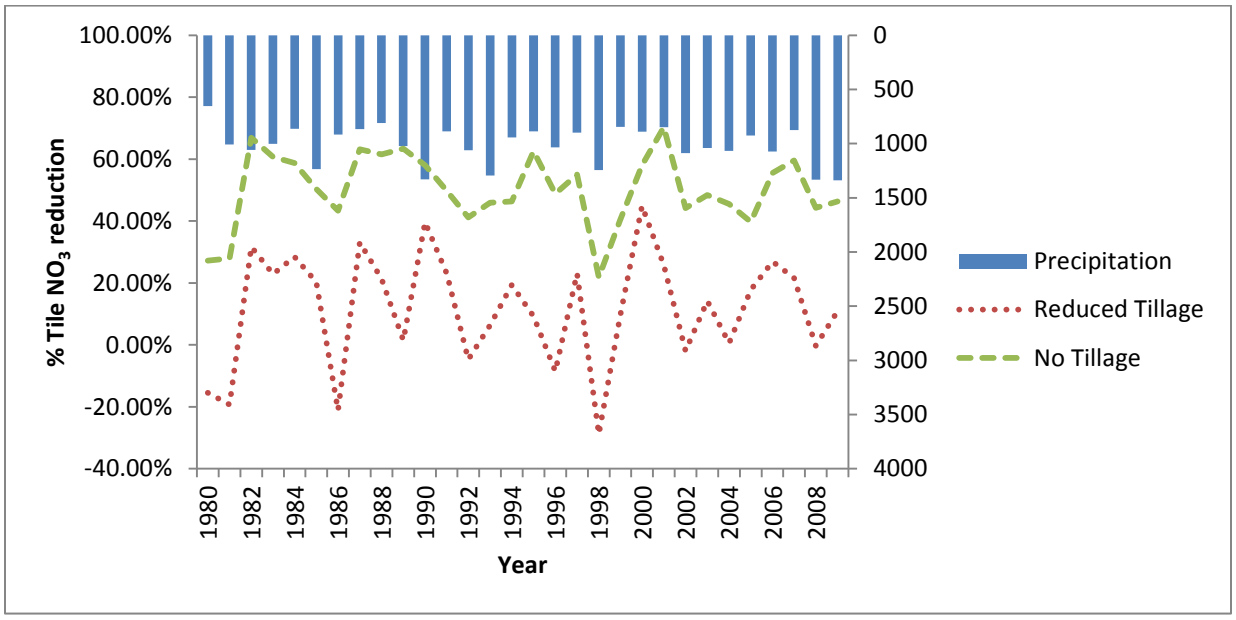

Figure 5.8. Nitrate load reduction in tile flow for different tillage practices compared to conventional tillage on annual basis (1980-2009).

5.2.2. Filter Strips

Though filter strips are a commonly used BMP, their usefulness in nutrient reduction in a tile-drained watershed is minimal. Since most of the nutrients are discharged via tile drainage instead of surface runoff, only a small amount of nutrients can be removed. Filter strip size does not significantly matter since only nitrate discharge in surface flow can be removed, and much of that is already removed with smaller filter strips (see Figure 5.9). In the Bosch et al (2013) study, the filter strip with a 25% trapping efficiency managed to remove about 14% of nitrogen discharged from surface flow. Sahu and Gu (2009) found some subbasins in their model of the Walnut Creek watershed in Iowa had upwards of 80% of nitrate removed in a normal year for filter strips with a ratio of 10 on a moderately well drained soil. Both of these studies used an older version of SWAT's filter strips routines and mainly dealt with non-tile drained areas when evaluating the filter strips.

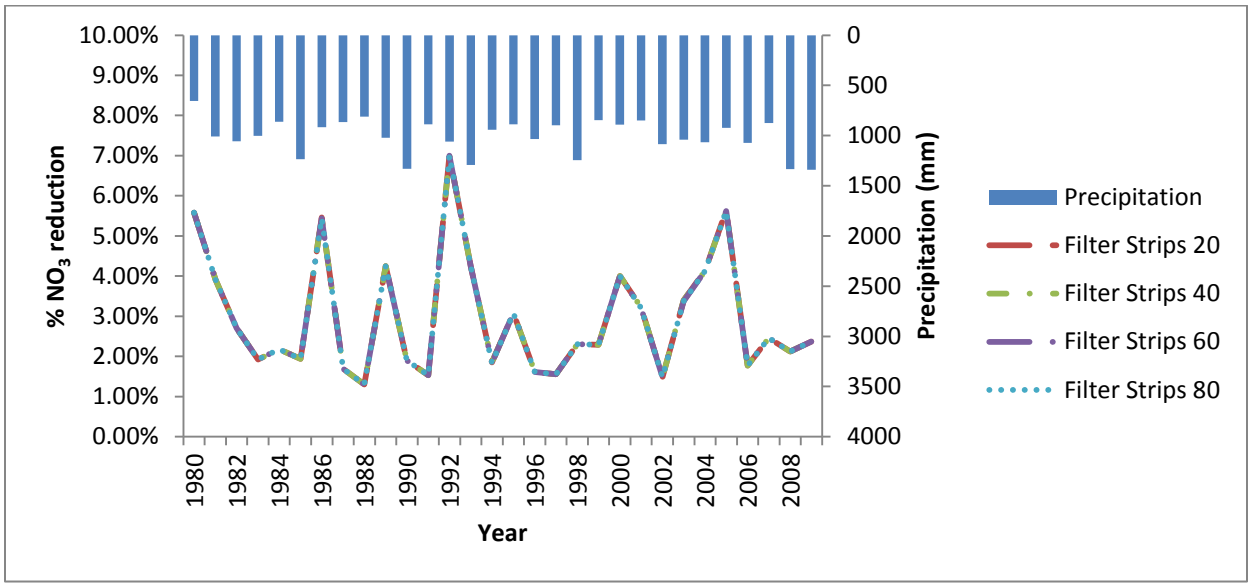

Figure 5.9. Nitrate load reduction in outlet flow for different filter strip configurations compared with no filter strip on annual basis (1980-2009).

5.2.3. Wetlands

Since only surface runoff is assumed by SWAT to enter the wetlands, nitrate reduction potential is limited. A larger surface area, rather than volume, is desirable for nitrate reduction because SWAT only assumes settling and no nutrient transformation occurs (see Figure 5.10). The master's thesis by Miller (1997) had reductions of about 35% due to tile drainage rather than surface runoff being collected and stored in the wetland.

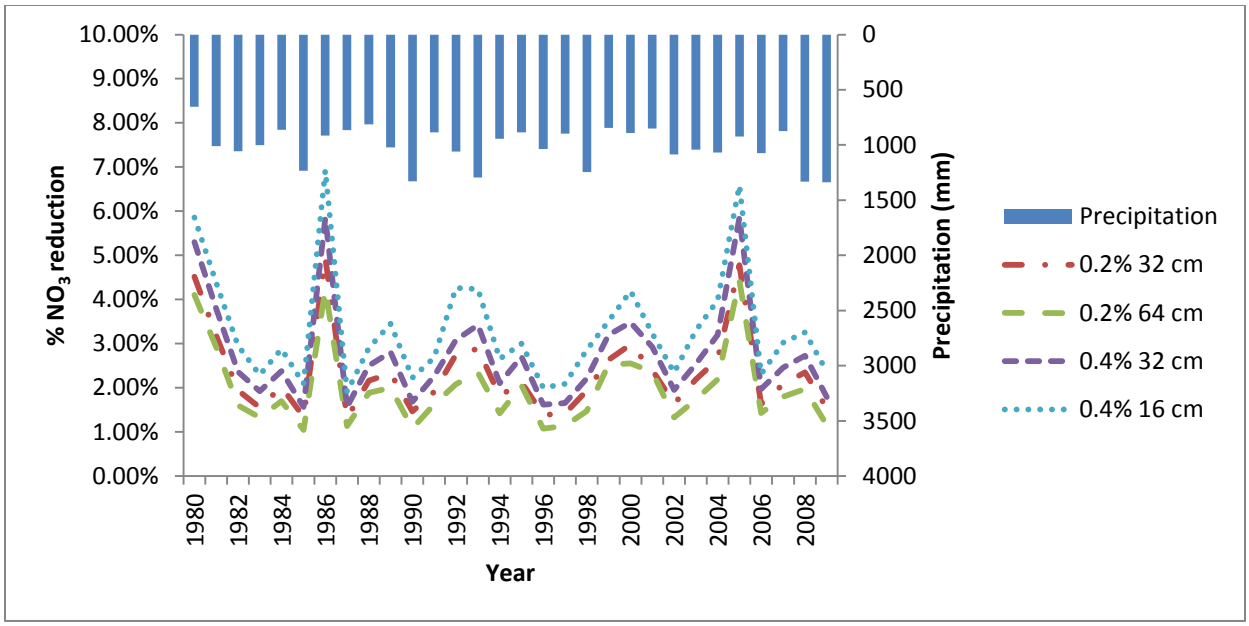

Figure 5.10. Nitrate load reduction in outlet flow for different wetland configurations compared with no wetland.

In investigating the effects that wetland restoration would have on water quality in the Little Saskatchewan River Conservation District, Wang et al.'s (2010) model simulated a reduction in both nitrogen and phosphorus reduction of up to 25% on an average annual basis with an increase of total area draining into wetlands of 3103 ha. Their first study watershed experiences a 120 m drop in elevation, with greater snowfall and a much colder climate than LVR. It also contains less agriculture than LVR and a different soil type. These factors are the reason why discharge from their study watershed is much lower than from LVR. Wang et al. (2010) concurrently developed a comparison model to simulate the effects of removing wetlands in a similar watershed based in Minnesota; the simulated results showed an increase of nitrogen

and phosphorus loading of 22% and 25%, respectively, which concur with the decrease from their other watershed. The larger pollutant load of LVR compared with these watersheds and the assumption that only the surface flow of LVR would flow through the wetland BMP could explain the differences between the studies.

5.2.4. Combined BMPs

Since filter strips and wetlands deal primarily with surface flow, adding them to the BMP of no tillage improves the reduction of nitrates discharged from LVR only several percentage points because there is no interaction with tile flow from which a vast majority of nitrates are discharged. (See Figure 5.11 for impact of multiple simultaneous BMPs on nitrate reduction)

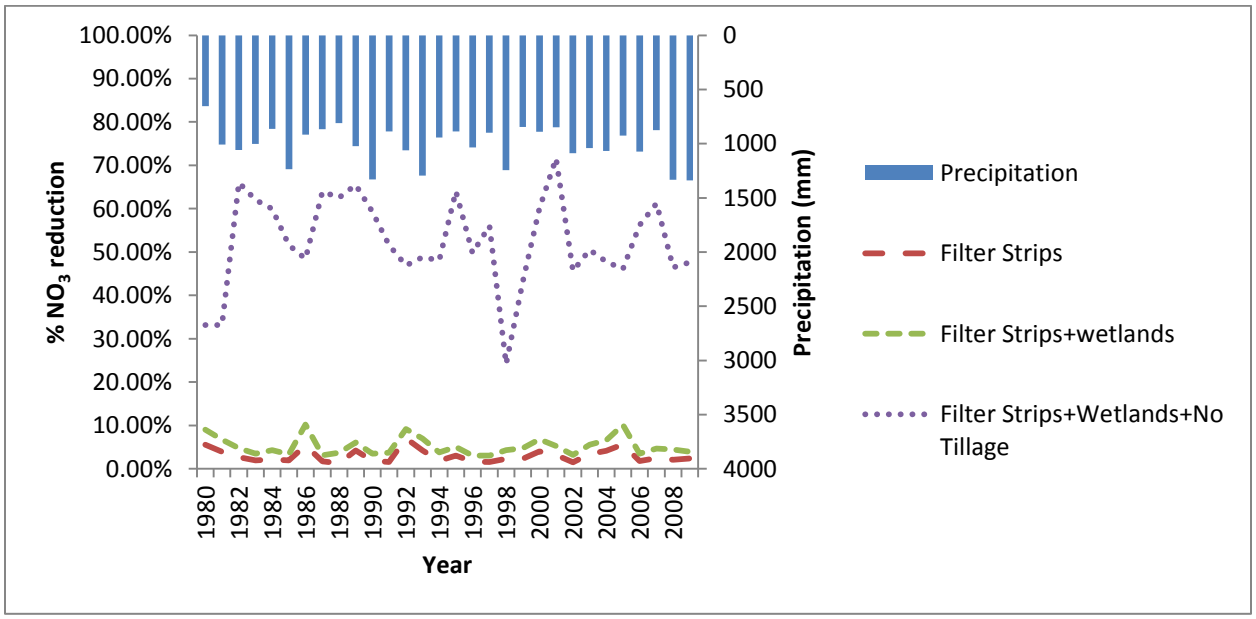

Figure 5.11. Additional impact on nitrate load reduction of multiple simultaneous BMPs.

5.3. Limitations

Since SWAT simplifies reality in order to model the hydrologic cycle, errors are created when the simplification does not match closely enough with reality. While SWAT removed

some land cover when creating HRUs, management practices were simplified by assuming uniformity throughout the watershed. This assumption could explain the inability of a calibration for mineral phosphorus.

The SWAT model also has a difficult time accurately modeling large storm events. In addition, sometimes the data measurements were not taken every day, leading to some days' data assumed to be equal to the last measured day's data.

Tile drainage does not flow into wetlands in the SWAT model. The primary purpose of wetlands in tile drainage watersheds is to remove nitrate discharge from the tile drainage before it enters the reach. The assumption of SWAT that tile drainage flow bypasses the wetlands leads to an underestimation of nitrate reduction.

6. Conclusions and Recommendations for future work

In order to determine the effectiveness of BMPs on the primarily tile-drained watershed LVR, a SWAT model was calibrated and validated on a daily basis using flow and nitrate discharge data from 1998-2000. SWAT CUP's SUFI routines modified the related parameters for multiple simulations and printed the best simulation (highest NS value) with the changed parameters and parameter sensitivity for the calibration period. The calibrated model was used to simulate each BMP on a yearly basis, assuming 100% implementation across the watershed.

Of the BMPs simulated, no tillage is the best individual BMP. By not disturbing the soil, macro pores are kept intact, allowing for preferential flow paths, improved root aeration, increased earthworm activity, and improved soil structure to occur. Though filter strips perform well in other watersheds, their effectiveness is minimal in a primarily tile-drained watershed. Wetlands reduce pollutants discharged from the watershed, but SWAT would require a modification so that tile flow could be stored in wetlands before entering the reach, allowing for simulated results closer to that of Miller (1997), as well as allowing nutrient transformation within the wetland.

One problem encountered was the limited amount of data available. Moriasa et al. (2007) stated that ideally calibration should include 3 to 5 years' worth of data and include a wet, dry, and average year in order for simulated model to be fitted to a large variety of hydrologic conditions, yet the data available encompassed a wet year followed by 2 dry years.

In future development of SWAT, the tile drainage needs to be enhanced by allowing for the discharge of other pollutants. Phosphorus can be discharged in tile drainage in trace amounts, something that the current version of SWAT does not calculate. A future version of

SWAT would need to allow other pollutants such as phosphorus to be discharged through tile drainage.

Though pesticides were also measured as a part of the original data, they were not looked at in this study. Lack of user knowledge about the active ingredients in the pesticides used by station farms combined with uncertainty of whether SWAT wants the amount of the pesticide mix applied or the total active ingredient mass in the mix; in addition, some pesticides which were used by the farm stations are not listed in the SWAT input/output documentation. These factors contributed to the decision not to calibrate and validate the model for them. A future study could look at these parameters in an attempt to further evaluate the BMPs.

By understanding the results of this study, County Extension offices in the immediate area of the study watershed would be able to use the results of this model to recommend to farmers methods of reducing nitrogen pollution discharged from their farms. Future studies of the Little Vermillion watershed should be able to use the calibrated and validated parameters from this study as a reference point, while concurrently providing a guideline to other watersheds in the region.

References

Algoazany, A.S. 2006. Long-term effects of agricultural chemicals and management practices on water quality in a subsurface drained watershed. Unpublished doctoral dissertation. Department of Agricultural and Biological Engineering, University of Illinois at Urbana-Champaign.

Arnold, J.G., P.M. Allen, and G. Bernhardt. 1993. A comprehensive surface—groundwater flow model. *J. Hydrology* 142(1-4): 47-69.

Arnold, J.G. and N. Fohrer. 2005. SWAT2000: current capabilities and research opportunities in applied watershed modeling. *Hydrological Processes* 19(3): 563-572.

Arnold, J.G., J.R. Kinley, R. Srinivasan, J.R. Williams, E.B. Haney, and S.L. Neitsch. 2012a. Soil & Water Assessment Tool Input/Output Documentation Version 2012. Texas Water Resources Institute.

Arnold, J.G., D.N. Moriasi, P.W. Gassman, K.C. Abbaspour, M.J. White, R. Srinivasan, C. Santhi, R.D. Harmel, A. van Griensven, M.W. Van Liew, N. Kannan, and M.K. Jha. 2012b. SWAT: Model use, calibration, and validation. *Transactions of the ASABE* 55(4): 1491-1508.

Arnold, J. G., R. Srinivasan, R. S. Muttiah, and J.R. Williams. 1998. Large-area hydrologic modeling and assessment: Part I. Model development. *J. American Water Resource Assoc.* 34(1): 73-89.

Arnold, J.G. and J.R. Williams. 1987. Validation of SWRRB—simulator for water resources in rural basins. *J. Water Resources Planning and Management* 113(2): 243-256.

Arnold, J.G. and J.R. Williams. 1995. SWRRB—A water scale model for soil and water resources management. p. 847-908. *In* V.P. Singh (ed) Computer models of watershed hydrology. Water Resources Publication.

Arnold, J.G., J.R. Williams, and D.R. Maidment. 1995. Continuous-time water and sediment-routing models for large basins. *J. Hydraulic Eng.* 121(2): 171-183.

Aulenbach, B. T., H. T. Buxton, W. A. Battaglin, and R. H. Coupe. 2007. Streamflow and nutrient fluxes of the Mississippi-Atchafalaya River basin and subbasins for the period of record through 2005. U.S. Geological Survey Open-File Report 2007-1080. (http://toxics.usgs.gov/pubs/of-2007-1080/ index.html).

Beasly, D.B., L.F. Huggins, and E.J. Monke. 1980. ANSWERS: A Model for Watershed Planning. *Trans. ASAE* 23(4): 938-944.

Benham, B.L., G. Yagow, I. Chaubey, and K.R. Douglas-Mankin. 2011. Advances in watershed management: modeling, monitoring, and assessment. Trans. ASABE 54(6): 2167-2170.

Bicknell, B.R., J.C. Imhoff, J.L. Kittle, Jr., A.S. Donigian, Jr., and R.C. Johanson. 1997. Hydrological Simulation Program—FORTRAN User's Manual for Version 11. AQUA TERRA consultants, Mountain View, California.

Bosch, D., F. Theurer, R. Bingner, G. Felton, and I. Chaubey. 2001. Evaluation of the AnnAGNPS water quality model. Southern cooperative series bulletin (45-54), Tifton, GA.

Bosch, N.S., J.D. Allen, J.P. Selegean, and D. Scavia. 2013. Scenario-testing of agricultural best management practices in Lake Erie watersheds. *J. Great Lakes Research* 39(3): 429-436.

Bouraoui, F. and T. A. Dillaha. 1996. ANSWERS-2000: Runoff and sediment transport model. *J. Environ. Eng.* 122(6): 493-502.

Bouraoui, F. and T. A. Dillaha. 2000. ANSWERS-2000: Non-point-source nutrient planning model. *J. Environ. Eng.* 126(11): 1045-1055.

Bouraoui, F. and B. Grizzetti. 2013. Modeling mitigation options to reduce nitrogen water pollution from agriculture. Science of the Total Environment (Article in Press).

Clean Water Act of December 1977, as amended; 33 U.S.C. 1151.

Chung, S.W., P.W. Gassman, R. Gu, and R.S. Kanwar. 2002. Evaluation of EPIC for assessing tile flow and nitrogen losses for alternative agricultural management systems. Trans. ASABE 45(4): 1135-1146.

Daniel, E. B., J. V. Camp, E. J. LeBeuf, J. R. Penrod, J. P. Dobbins and M. D. Abkowitz. 2011. Watershed modeling and its applications: A state-of-the-art review. Open Hydrology J. 5: 26-50.

Douglas-Mankin, K.R., R. Srinivasan, and J.G. Arnold. 2010. Soil and Water Assessment Tool (SWAT) model: current developments and applications. Trans. ASABE 53(5): 1423-1431.

Engel, B.A., R. Srinivasan, J. Arnold, C. Rewerts, and S.J. Brown. 1993. Nonpoint source (NPS) pollution modeling using models integrated with Geographic Information Systems (GIS). *Water Science & Tech* 28(3-5): 685-690.

Ficklin, D.L. and M. Zhang. 2013. A Comparison of the Curve Number and Green-Ampt Models in an Agricultural Watershed. Trans. ASABE 56(1): 61-69.

Francesconi, W., D.R. Smith, G.C. Heathman, X. Wang, and C.O. Williams. 2014. Monitering and APEX modeling of no-till and reduced-till in tile-drained agricultural landscapes for water quality. Trans. ASABE 57(3): 777-789.

Gassman, P. W., M. R. Reyes, C. H. Green, and J. G. Arnold. 2007. The Soil and Water Assessment Tool: Historical development, applications, and future research. *Trans. ASABE* 50(4): 1211-1240.

Gollamudi, A., C. A. Madramootoo, and P. Enright. 2007. Water quality modeling of two agricultural fields in southern Quebec using SWAT. *Trans. ASABE* 50(6): 1973-1980.

Hargreaves, G.L., G.H. Hargreaves, and J.P. Riley. 1985. Agricultural Benefits for Senegal River Basin. *J. Irrig. and Dain. Engr.* 108(3):225-230.

Hegesh, E. and J. Shiloah. 1982. Blood nitrates and infantile methemogobinemia. *Clinica Chimica Acta.* 125(2): 107-115.

Hooghoudt, S.B. 1940. Bijdragen tot de kenins wan enige natuurkundige groothenden va de ground. No. 7. Versl. Landbouwk. Onderz. (Contributions to the knowledge of some physical constants of the soil. No. 7. Report Agricultural Research). 46: 515-707.

Izaurralde, R.C., J.R. Williams, W.B. McGill, N.J. Rosenberg, and M.C. Quirroga Jakas. 2006. Simulating soil C dynamics with EPIC: Model description and testing against long-term data. *Ecol. Model.* 192(3-4): 362-384.

Jones, C.A., C.V. Cole, A.N. Sharpley, and J.R. Williams. 1984. A simplified soil and plant phosphorus model. I. Documentation. *Soil Sci. Soc. Am. J.* 48:800-805.

King, K.W., J.G. Arnold, and R.L. Bingner. 1999. Comparison of Green-Ampt and Curve Number Methods on Goodwin Creek Watershed Using SWAT. Trans. ASAE 42(4): 919-925.

Kirkham, D. 1957. Theory of land drainage. *In* "Drainage of Agricultural Lands Agronomy Monograph No. 7." Madison, WI: American Society of Agronomy.

Knisel, W.G. 1980. CREAMS, a field-scale model for chemicals, runoff, and erosion from agricultural management systems. USDA Conservation Research Report No. 26. Washington, D.C.: USDA.

Krysanova, V., D.-I. Müller-Wohlfeil, and A. Becker. 1998. Development and test of a spatially distributed hydrological/water quality model for mesoscale watersheds. *Ecological Modeling* 106(2-3): 261-289.

Laflen, J.M., L.J. Lane, and G.R. Foster. 1991. WEPP: A new generation of erosion prediction technology. *J. Soil and Water Conservation* 46(1): 34-38.

Lee, Y.W., M.F. Dahab, and I. Bogardi. 1995. Nitrate-Risk Assessment Using Fuzzy-Set Approach. *J. Environ. Eng.* 121(3): 245-256.

Leonard, R.A., W.G. and D.A. Still. 1987. GLEAMS: Groundwater loading effects of agricultural management systems. *Trans. ASAE* 30(5): 1403-1418.

Lenhart, T., K. Eckhardt, N. Fohrer, and. H.-G. Frede. 2002. Comparison of two different approaches of sensitivity analysis. *Physics and Chemistry of the Earth* 27(9-10): 645-654.

Miller, P.S. 1997. An analysis of constructed wetlands performance: A concentration and mass load assessment. Unpublished Master's Thesis. Department of Agricultural and Biological Engineering, University of Illinois at Urbana-Champaign.

Mirvish, S.S. 1991. The significance for human health of nitrate, nitrite, and N-nitroso compounds. *Nitrate contamination: exposure, consequences and control*. I. Bogardi and R.D. Kuzelka, eds., Springer-Verlag, Berlin, Germany, 253-266.

Mohamoud, Y. M. 2007. Enhancing Hydrological Simulation Program-Fortran model channel hydraulic representations. *J. American Water Resources Association* 43(5): 1280-1292.

Moriasi, D.N., C.G. Rossi, J.G. Arnold and M.D. Tomer. 2012. Evaluating hydrology of the Soil and Water Assessment Tool (SWAT) with new tile drain equations. *Journal of Soil and Water Conservation* 67(6): 513-524.

Nash, J. E., and J. V. Sutcliffe, 1970. River Flow Forecasting through Conceptual Models 1. A Discussion of Principles. *Journal of Hydrology* 10(3): 282-290.

Neitsch, S.L., J.G. Arnold, J.R. Kiniry, and J.R. Williams. 2009. Soil and Water Assessment Tool Theoretical Documentation. Version 2009. Temple Tex.: USDA-ARS Grassland, Soil, and Water Research Laboratory, Blackland Research Center, Texas Agricultural Experiment Station.

Nitrates and drinking water. 1988. *Tech. Rep. No. 27.* European Industry and Toxicology Centre, Brussels, Belgium.

Osterman, L.E., R.Z. Poore, P. W. Swarzenski, D.B. Senn, and S.F. DiMarco. 2009. The 20th-century development and expansion of Louisiana shelf hypoxia, Gulf of Mexico. *Geo-Marine Letters* 29(6): 405-414.

Rabotyagov, S., T. Campbell, M. Jha, P.W. Gassman, J. Arnold, L. Kurkalova, S. Secchi, H. Feng, and C.L. Kling. 2010. Least-cost control of agricultural nutrient contributions to the Gulf of Mexico hypoxic zone. *Ecological Applications* 20(6): 1542-1555.

Rallison, R.E. and N. Miller. 1981. Past, present, and future SCS runoff procedure. p. 353-364. *In* V.P. Singh (ed.). Rainfall runoff relationship. Water Resources Publication, Littleton, CO.

Rast, W. and G.F. Lee. 1973. Summary Analysis of the North American project (US portion) OECD eutrophication project: nutrient loading-lake response relationships and trophic state indices. USEPA Corvallis Environmental Research Laboratory, Corvallis, OR. EPA-600/3-78-008.

Sahu, M and R.R. Gu. 2009. Modeling the effects of riparian buffer zone and contour strips on stream water quality. *Ecological Eng.* 35(8): 1167-1177.

Saleh, A. and O. Gallego. 2007. Application of SWAT and APEX using the SWAPP (SWAT-APEX) program for the Upper North Bosque River Watershed in Texas. *Trans. ASABE* 50(4): 1177-1187.

Soil Conservation Service. 1972. Section 4: Hydrology *In* National Engineering Handbook. SCS.

Tan, C.S, C.F. Drury, M. Soultani, I.J. van Wesenbeeck, HYF Ng, JD Gaynor, and TW Welacky. 1998. Effect of controlled drainage and tillage on soil structure and tile drainage nitrate loss at the field scale. Water science and technology 38 (4-5): 103-110.

Thomas, R.E. and S.C. Reed. 1980. EPA Policy on Land Treatment and the Clean Water Act of 1977. *J. Water Pollution Control Federation* 52(3) part 1: 452-460.

Thornthwaite, C.W. 1948. An approach towards a rational classification of climate. Geographical Review 38:55-94.

Tiwari, A.K, L.M. Risse, M.A. Nearing. 2000. Evaluation of WEPP and its comparison with USLE and RUSLE. *Trans. ASAE* 43(5): 1129-1135.

Wang, X., S. Shang, Z. Qu, T. Liu, A.M. Melesse, W. Yang. 2010. Simulated wetland conservation-restoration effects on water quantity and quality at watershed scale. *J. Env. Management* 91: 1511-1525.

White, M.J. and J.G. Arnold. 2009. Development of a simplistic vegetative filter strip model for sediment and nutrient retention at the field scale. *Hydrological Processes* 23: 1602-1616.

Wilcoxon, F. 1945. Individual Comparison by Ranking Methods. *Biometrics Bulletin* 1(6): 80-83. Stable URL: http://www.jstor.org/stable/3001968 accessed 11/20/13

Williams, J.R. 1990. The erosion productivity impact calculator (EPIC) model: A case history. *Phil. Trans. R. Soc. London* 329(1255): 421-428

Williams, J.R. 1995. Chapter 25: The EPIC model. p. 909-1000. *In* V.P. Singh (ed.). Computer models of watershed hydrology. Water Resources Publication, Highlands Ranch, CO.

Winchell, M., R. Srinivasan, M. Di Luzio, and J. Arnold. 2010. ArcSWAT Interface for SWAT2009. Temple Tex.: USDA-ARS Grassland, Soil, and Water Research Laboratory, Blackland Research Center, Texas Agricultural Experiment Station.

Wischmeier, W.H., C.B. Johnson, and B.V. Cross. 1971. A soil erodibilty nomograph for farmland and construction sites. *J. Soil and Water Conservation* 26:189-193.

Wischmeier, W.H. and D.D. Hunter. 1978. Predicting rainfall erosion losses: a guide to conservation planning. Agriculture Handbook. USDA-ARS

Young, R.A., C.A. Onstad, D.D. Bosch, and W.P. Anderson. 1998. AGNPS: A nonpoint-source pollution model for evaluating agricultural watersheds. *J. Soil and Water Conservation* 44(2): 168-173.

Zhang, X.C., M.A. Nearing, L.M. Risse, and K.C. McGregor. 1996. Evaluation of WEPP runoff and soil loss predictions using natural runoff plot data. *Trans. ASAE* 39(3): 855-863.

Zhao, P., B. Xia, Y. Hu, and Y. Yang. 2013. A spatial multi-criteria planning scheme for evaluating riparian buffer restoration priorities. *Ecological Engineering* 54: 155-164.

Appendix A

Table A-1. Land use distribution percentage before and after HRU definition

Land use	Before definition percentage	After definition percentage
Corn-Soybean	32.33%	48.79%
Soybean-Corn	32.34%	48.93%
Urban	3.72%	1.96%
Water	0.12%	0.12%
Forest	2.33%	0.2%
Wetlands	0.03%	0%
Hay	1.57%	0 %
Other Agriculture	25.40%	0%

Table A-2. Soil series distribution percentage before and after HRU definition

Soil series	Soil Texture	Before definition percentage	After definition percentage
Catlin	Silt Loam	2.9%	1.3%
Dana	Silt Loam	5.4%	4.1%
Drummer	Silty Clay Loam	43%	53%
Elburn	Silt Loam	3.2%	1.7%
Flanagan	Silt Loam	26%	32%
Pella	Clay Loam	2.7%	1.9%
Plano	Silt Loam	1.2%	0.81%
Raub	Silt Loam	4.9%	5.4%
Sabina	Silt Loam	2.6%	0.60%
Xenia	Silt Loam	1.4%	0.13%
Other		6.4%	0.78%

Appendix B

B.1. Conventional Tillage

Table B-1. Assumed conventional Corn-Soybean Rotation

Year & Date	Management Operation
March 14, Year 1	Ammonia applied to surface at 224 kg/ha
April 16, Year 1	Field Cultivator Tillage operation
April 16, Year 1	Plant Corn/Begin growing season
June 15, Year 1	Row Cultivator Tillage operation
September 8, Year 1	Harvest Corn/End growing season
September 15, Year 1	V-ripper Tillage operation
May 22, Year 2	Field Cultivator Tillage operation
May 23, Year 2	Plant Soybean/Begin growing season
October 13, Year 2	Harvest Soybeans/End growing season
November 4, Year 2	00-46-00 applied to surface at 484 kg/ha
November 5, Year 2	V-ripper Tillage operation
April 1, Year 3	Ammonia applied to surface at 202 kg/ha
April 13, Year 3	Field Cultivator Tillage operation
April 14, Year 3	Plant Corn/Begin growing season
June 5, Year 3	Row Cultivator Tillage operation
October 8, Year 3	Harvest Corn/End growing season
April 12, Year 4	Field Cultivator Tillage operation
May 15, Year 4	Field Cultivator Tillage operation
May 16, Year 4	Plant Soybean/Begin growing season
September 29, Year 4	Harvest Soybean/End growing season
September 30, Year 4	08-20-27 applied to surface at 336 kg/ha
October 5, Year 4	V-ripper Tillage operation
March 19, Year 5	Ammonia applied to surface at 207 kg/ha
April 11, Year 5	Field Cultivator Tillage Operation
April 12, Year 5	Plant Corn/Begin growing season
September 14, Year 5	Harvest Corn/End growing season
September 23, Year 5	03-10-41 applied to surface at 149 kg/ha
September 25, Year 5	V-ripper Tillage operation
March 6, Year 6	Field Cultivator Tillage operation
April 28, Year 6	Field Cultivator Tillage operation
April 29, Year 6	Plant Soybean/Begin growing season
Junk 15, Year 6	Row Cultivator Tillage operation
September 15, Year 6	Harvest Soybean/End growing season
September 18, Year 6	08-20-27 applied to surface at 390 kg/ha
September 20, Year 6	V-ripper Tillage operation

Table B-2. Assumed Conventional Soybean-Corn Rotation.

Year & Date	Management Operation
June 3, Year 1	Field Cultivator Tillage operation
June 4, Year 1	Plant Soybean/Begin growing season
July 5, Year 1	Row Cultivator Tillage operation
October 2, Year 1	Harvest Soybean/End growing season
October 5, Year 1	08-20-27 applied to surface at 289 kg/ha
October 6, Year 1	V-ripper Tillage operation
April 9, Year 2	Ammonium applied to surface at 197 kg/ha
April 17, Year 2	Field Cultivator Tillage operation
April 18, Year 2	Plant Corn/Begin growing season
September 19, Year 2	Harvest Corn/End growing season
September 20, Year 2	03-10-41 applied to surface at 168 kg/ha
September 21, Year 2	V-ripper Tillage operation
April 23, Year 3	Field Cultivator Tillage operation
April 26, Year 3	Field Cultivator Tillage operation
April 29, Year 3	Play Soybean/Begin growing season
July 1, Year 3	Row Cultivator Tillage operation
September 26, Year 3	Harvest Soybean/End growing season
September 27, Year 3	08-20-27 applied to surface at 448 kg/ha
April 17, Year 4	Ammonium applied to surface at 164 kg/ha
April 25, Year 4	Field Cultivator Tillage operation
April 26, Year 4	Plant Corn/Begin growing season
September 23, Year 4	Harvest Corn/End growing season
September 24, Year 4	03-10-41 applied to surface at 224 kg/ha
September 25, Year 4	V-ripper Tillage operation
April 14, Year 5	Field Cultivator Tillage operation
May 6, Year 5	Field Cultivator Tillage operation
May 7, Year 5	Plant Soybean/Begin growing season
June 15, Year 5	Row Cultivator Tillage operation
September 19, Year 5	Harvest Soybean/End growing season
September 20, Year 5	06-13-34 applied to surface at 308 kg/ha
September 22, Year 5	V-ripper Tillage operation
March 3, Year 6	Ammonium applied to surface at 151 kg/ha
April 12, Year 6	Field Cultivator Tillage Operation
April 13, Year 6	Plant Corn/Begin growing season
September 19, Year 6	Harvest Corn/Begin growing season
September 28, Year 6	06-15-34 applied to surface at 280 kg/ha
October 2, Year 6	V-ripper Tillage operation

B.2. Reduced Tillage

Table B-3. Assumed Corn-Soybean Reduced Tillage operations

Year & Date	Management Operation
March 14, Year 1	Anhydrous Ammonia applied to surface at 224 kg/ha
April 15, Year 1	Field Cultivator Tillage
April 16, Year 1	Plant Corn/Begin Growing Season
September 8, Year 1	Harvest Corn/End Growing Season
September 15, Year 1	V-ripper tillage
May 22, Year 2	Field Cultivator Tillage
May 23, Year 2	Plant Soybean/Begin Growing Season
October 13, Year 2	Harvest Soybean/End Growing Season
November 4, Year 2	00-46-00 applied to surface at 483.46 kg/ha
November 5, Year 2	V-ripper tillage
April 1, Year 3	Anhydrous Ammonia applied to surface at 201.6 kg/ha
April 13, Year 3	Field Cultivator Tillage
April 14, Year 3	Plant Corn/Begin Growing season
June 5, Year 3	Row Cultivator Tillage
October 8, Year 3	Harvest Corn/End Growing season
April 12, Year 4	Field Cultivator Tillage
May 15, Year 4	Field Cultivator Tillage
May 16, Year 4	Plant Soybean/Begin Growing Season
September 29, Year 4	Harvest Soybean/End Growing Season
September 30, Year 4	08-20-27 applied to surface at 336 kg/ha
October 5, Year 4	V-ripper tillage
March 19, Year 5	Anhydrous Ammonia applied to surface at 207 kg/ha
April 12, Year 5	Field Cultivator Tillage
April 12, Year 5	Plant Corn/Begin Growing season
September 22, Year 5	Harvest Corn/End Growing Season
September 23, Year 5	03-10-41 applied to surface 126.56 kg/ha
September 25, Year 5	V-ripper Tillage
March 6, Year 6	Field Cultivator Tillage
April 28, Year 6	Field Cultivator Tillage
April 29, Year 6	Plant Soybean/Begin Growing season
June 6, Year 6	Row Cultivator Tillage
September 15, Year 6	Harvest Soybean/End Growing season
September 18, Year 6	08-20-27 applied to surface at 389.76 kg/ha
September 19, Year 6	V-ripper tillage

Table B-4. Assumed Soybean-Corn Reduced Tillage Operations

Year & Date	Management Operation
June 4, Year 1	Field Cultivator Tillage
June 4, Year 1	Plant Soybean/Begin Growing season
July 10, Year 1	Row Cultivator Tillage
October 4, Year 1	Harvest Soybean/End Growing season
October 5, Year 1	08-20-27 applied to surface at 289 kg/ha
October 6, Year 1	V-ripper Tillage
April 8, Year 2	Anhydrous Ammonia applied to surface at 224 kg/ha
April 17, Year 2	Field Cultivator Tillage
April 18, Year 2	Plant Corn/Begin Growing season
September 19, Year 2	Harvest Corn/End Growing season
September 20, Year 2	03-10-41 applied to surface at 168 kg/ha
September 21, Year 2	V-ripper Tillage
April 23, Year 3	Field Cultivator Tillage
April 26, Year 3	Field Cultivator Tillage
April 29, Year 3	Plant Soybean/Begin Growing season
July 1, Year 3	Row Cultivator Tillage
September 26, Year 3	Harvest Soybean/End Growing Season
September 27, Year 3	08-20-27 applied to surface at 448 kg/ha
April 19, Year 4	Anhydrous Ammonia applied to surface at 164 kg/ha
April 25, Year 4	Field Cultivator Tillage
April 26, Year 4	Plant Corn/Begin Growing season
September 23, Year 4	Harvest Corn/End Growing season
September 24, Year 4	03-10-41 applied to surface at 224 kg/ha
September 25, Year 4	V-ripper Tillage
April 14, Year 5	Field Cultivator Tillage
May 6, Year 5	Field Cultivator Tillage
May 7, Year 5	Plant Soybean/Begin Growing season
June 15, Year 5	Row Cultivator Tillage
September 19, Year 5	Harvest Soybean/End Growing season
September 20, Year 5	06-13-34 applied to surface at 308 kg/ha
September 22, Year 5	V-ripper Tillage
March 8, Year 6	Anhydrous Ammonia applied to surface at 183.68 kg/ha
April 12, Year 6	Field Cultivator Tillage
April 13, Year 6	Plant Corn/Begin Growing Season
September 19, Year 6	Harvest Corn/End Growing Season
September 28, Year 6	06-15-34 applied to surface at 280 kg/ha
October 2, Year 6	V-ripper tillage

B.3. No Tillage

Table B-5. Assumed Corn-Soybean No Tillage operations

Year & Date	Management Operation
May 5, Year 1	Plant Corn/Begin Growing season
June 13, Year 1	Anhydrous Ammonia applied to surface at 173.6 kg/ha
October 17, Year 1	Harvest Corn/End Growing season
June 25, Year 2	Plant Soybean/Begin Growing season
October 17, Year 2	Harvest Soybean/End Growing season
April 4, Year 3	09-23-30 applied to surface at 448 kg/ha
April 23, Year 3	Plant Corn/Begin Growing season
June 6, Year 3	00-06-00 applied to surface at 106.4 kg/ha
October 14, Year 3	Harvest Corn/End Growing season
May 29, Year 4	Plant Soybean/Begin Growing season
September 28, Year 4	Harvest Soybean/End Growing season
March 11, Year 5	09-23-30 applied to surface at 448 kg/ha
April 29, Year 5	Plant Corn/Begin Growing Season
June 1, Year 5	Anhydrous Ammonia applied to surface at 114.16 kg/ha
November 9, Year 5	Harvest Corn/End Growing season
May 16, Year 6	Plant Soybean/Begin Growing season
October 4, Year 6	Harvest Soybean/End Growing season

Table B-6. Assumed Soybean-Corn No till management operations.

Year & Date	Management Operation
June 6, Year 1	Plant Soybean/Begin Growing Season
September 26, Year 1	Harvest Soybean/End Growing Season
May 21, Year 2	Plant Corn/Begin Growing Season
June 26, Year 2	Anhydrous Ammonia applied to surface at 174 kg/ha
November 12, Year 2	Harvest Corn/End Growing Season
May 17, Year 3	Plant Soybean/Begin Growing season
October 4,Year 3	Harvest Soybean/End Growing Season
March 30, Year 4	09-23-30 applied to surface at 448 kg/ha
April 27, Year 4	Plant Corn/Begin Growing Season
June 11, Year 4	Anhydrous Ammonia applied to surface at 123 kg/ha
October 24, Year 4	Harvest Corn/End Growing Season
May 20, Year 5	Plant Soybean/Begin Growing season
September 24, Year 5	Harvest Soybean/End Growing Season
March 8, Year 6	09-23-30 applied to surface at 448 kg/ha
April 26, Year 6	Plant Corn/Begin Growing season
May 31, Year 6	Anhydrous Ammonia applied to surface at 119 kg/ha
November 14, Year 6	Harvest Corn/End Growing season